ASCE

Accounting for Intrinsic Soil Properties and State Variables on Liquefaction Triggering

Russell A. Green, F.ASCE[1]; Aaron S. Bradshaw, M.ASCE[2]; and Christopher D. P. Baxter, M.ASCE[3]

Abstract: This paper proposes a new approach for incorporating the positive attributes of the small-strain shear wave velocity (V_S), stress-based simplified procedure and the cyclic strain procedure into penetration test, stress-based simplified liquefaction triggering models, with the objective of more fully accounting for the influence of intrinsic soil properties and soil state variables on liquefaction triggering. Current simplified liquefaction procedures are limited in their ability to capture the effects of intrinsic properties (grain size, mineralogy, grain shape, etc.) and the state properties (stress state, void ratio, fabric, etc.). To overcome these limitations, a new mechanistically based K_γ factor is proposed that can be incorporated in penetration test, stress-based simplified liquefaction triggering models in place of the currently used K_σ factor. However, K_γ is conceptually very different from K_σ. While most K_σ relationships have largely been empirically based and relate to the soil's cyclic resistance to liquefaction, K_γ is more mechanistically based and relates to the loading imposed on the soil. Specifically, K_γ is based on equating the shear strain induced in a given soil at given initial stress state and subjected to a given shear stress to the induced shear strain when the soil is confined at a reference initial stress state, all else being equal. Analyses show that K_γ is able to capture the liquefaction triggering behavior in both lab and field data in a wide range of soils and stress states. Numerically, K_γ and K_σ are similar for young, normally consolidated sandy soils when the factor of safety (FS) against liquefaction triggering is close to one, but may differ significantly for other scenarios and/or conditions. This has important implications for probabilistic-based analyses which consider a range of shaking intensities imposed on the soil, not just the case where $FS = 1$. **DOI: 10.1061/(ASCE)GT.1943-5606.0002823.** © *2022 American Society of Civil Engineers.*

Introduction

Liquefaction triggering is the result of the contractive tendencies in sandy soils when shaken, resulting in the progressive to rapid breakdown of the soil skeleton and the consequential transfer of the overburden stress from the soil skeleton to the pore fluid. This leads to an increase in excess pore water pressure and a reduction in soil stiffness and strength. The semiempirical, stress-based simplified procedure was originally proposed independently by Whitman (1971), and Seed and Idriss (1971), and is the most commonly used approach for evaluating liquefaction triggering worldwide. The procedure has continually evolved and has been updated as a result of the compilation of additional field case histories and trends identified in laboratory and numerical parametric studies (e.g., Tokimatsu and Yoshimi 1983; Seed 1983; Cetin et al. 2000, 2004; Boulanger 2003; Moss et al. 2003; Idriss and Boulanger 2008; Boulanger and Idriss 2014; Cetin and Bilge 2015; Lasley et al. 2016, 2017; Green et al. 2014, 2019, 2020; Wood et al. 2017; Ulmer et al. 2022; among many others). Additionally, variants of the procedure have been proposed wherein the soil's cyclic resistance to liquefaction, quantified in terms of Cyclic Resistance Ratio (CRR), is correlated to normalized Standard Penetration Test (SPT) blow count ($N_{1,60cs}$) (e.g., Cetin et al. 2000, 2004), normalized Cone Penetration Test (CPT) tip resistance (q_{c1Ncs}) (e.g., Moss et al. 2003), or normalized small-strain shear wave velocity (V_{S1}) (e.g., Kayen et al. 2013), among other normalized in-situ test measurements. Whitman (1971) and Seed (1976, 1979) recognized the significance of intrinsic soil properties and soil state variables on liquefaction triggering. In this context, intrinsic soil properties include the mineralogy, size, shape, surface characteristics, and gradation of the soil particles, and soil state variables include particle arrangement and packing (i.e., fabric and relative density), cementation, and stress state (e.g., Salgado et al. 1997; Mitchell and Soga 2005). Whitman (1971) and Seed (1976, 1979) assumed that penetration resistance is similarly influenced by these factors as CRR is, such that correlations between normalized penetration resistance and CRR sufficiently account for the influence of intrinsic soil properties and soil state variables on liquefaction triggering. However, this has been shown not to be completely the case.

Subsequent studies have shown that small-strain shear wave velocity (V_S) is also a function of many of the intrinsic soil properties and soil state variables that influence liquefaction triggering (e.g., Dobry et al. 1981; Tokimatsu et al. 1986; Tokimatsu and Uchida 1990), although the sensitivity of V_S to some of these properties or variables has been questioned (e.g., Verdugo 2016). Nevertheless, several stress-based correlations have been developed relating normalized V_S (i.e., V_{S1}) to CRR (e.g., Stokoe et al. 1988; Andrus et al. 2004; Kayen et al. 2013), similar to the correlations relating normalized penetration resistance (e.g., $N_{1,60cs}$ or q_{c1Ncs}) to CRR.

Despite the popularity of the stress-based procedures, multiple studies have shown that excess pore water pressure development better correlates to cyclic shear strain than to cyclic stress (e.g., Martin et al. 1975; Dobry et al. 1982; Byrne 1991). The reason for this is that the relative movement of soil particles during

[1]Professor, Dept. of Civil and Environmental Engineering, Virginia Tech, Blacksburg, VA 24061 (corresponding author). ORCID: https://orcid.org/0000-0002-5648-2331. Email: rugreen@vt.edu

[2]Associate Professor, Dept. of Civil and Environmental Engineering, Univ. of Rhode Island, Kingston, RI 02881.

[3]Professor, Dept. of Ocean Engineering, Univ. of Rhode Island, Kingston, RI 02881.

Note. This manuscript was submitted on March 23, 2021; approved on March 10, 2022; published online on May 11, 2022. Discussion period open until October 11, 2022; separate discussions must be submitted for individual papers. This paper is part of the ***Journal of Geotechnical and Geoenvironmental Engineering***, © ASCE, ISSN 1090-0241.

shear, which is necessary for breaking down the soil skeleton and the generation of excess pore water pressures, relates to the induced strain, regardless of amplitude of the stress applied to the soil. In this vein, Dobry et al. (1982) proposed the cyclic strain procedure as an alternative to stress-based approaches to evaluate liquefaction triggering. Although this procedure generally received a positive reception by liquefaction researchers because it largely circumvents the need to account for intrinsic soil properties and soil state variables on liquefaction triggering, the procedure has never been widely embraced by practice. Nevertheless, the Dobry et al. (1982) strain-based procedure highlights the role of soil shear stiffness (e.g., V_S) in evaluating liquefaction triggering when loading is quantified in terms of shear stress, τ, because V_S (or the corresponding small-strain shear modulus, $G_{\max}$) is the link to the induced strain (e.g., Dobry and Abdoun 2015a).

Proposed herein is an approach that better accounts for the influence of intrinsic soil properties and soil state variables on both the loading and the soil's cyclic resistance to liquefaction by incorporating V_S into stress-based penetration-resistance triggering models, in line with similar proposals by Hayati and Andrus (2009), Robertson (2015), and Jefferies and Been (2016). This is done through a newly-proposed, more mechanistically-based K_γ factor, which would replace the K_σ factor in future-developed stress-based simplified models. K_γ is based on equating the shear strain induced in a given soil at given initial stress state and subjected to a given shear stress to that induced when the soil is confined at a reference initial stress state, all else being equal. Central to the K_γ factor is the inter-relationship among the influence of effective confining stress on the contractive/dilative tendencies of the soil and the soil stiffness, the amplitude of imposed shear stress and the soil stiffness on the induced shear strain, and the amplitude of the induced shear strain and the contractive/dilative tendencies of the soil on the excess pore water pressure generation. K_γ is conceptually very different from most K_σ relationships, which have been largely empirically based and relate the ability of a given soil confined at a given stress state to resist liquefaction triggering to that of the same soil confined at a reference stress state. Because K_γ relates to the influence of the intrinsic soil properties and soil state variables on the applied loading, penetration resistance can still be used as an index for the influence of these factors on the soil's ability to resist liquefaction.

In the following, summaries of relevant studies are presented on liquefaction triggering, where loading is quantified in terms of either shear stress or shear strain. Based on the findings from these studies, the conceptual basis for K_γ is then presented. This is followed by direct validation, and broader implications and corollary validation of the K_γ-concept. It is the validation from multiple perspectives that provides the strong credence of the K_γ-concept, because if the validation from any one perspective does not hold, the overall K_γ-concept does not hold. The conceptual differences between K_γ versus K_σ are then discussed, the K_γ relationship is compared and contrasted to select K_σ relationships, and scenarios where the K_γ versus K_σ can lead to different predictions are discussed.

Influence of Intrinsic Soil Properties and Soil State Variables on Liquefaction Triggering

Stress-Based Studies

Several studies have examined the influence of soil fabric on liquefaction resistance. Two of the earliest studies were by Mulilis et al. (1975, 1977) who examined the influence of sample preparation methods on liquefaction resistance of soil. Mulilis et al. (1975, 1977) present the results from stress-controlled cyclic triaxial tests performed on samples of Monterey sand prepared using 11 different techniques. All the samples were prepared to a relative density (D_r) of 50% and confined at initial isotropic effective stress (σ_o') of 55.2 kPa. Because the samples were prepared using different techniques, they inherently had different particle arrangements and, thus, different fabrics. However, the intrinsic properties of the soil used and all other soil state variables were held the same. The results are shown in Fig. 1 and highlight the significant influence of fabric on a soil's cyclic resistance to liquefaction, where liquefaction was defined as pore water pressure equaling the initial effective confining stress or axial strains reaching ±2.5%, which occurred at approximately the same number of cycles.

A similar study was performed by Tokimatsu and Uchida (1990) who prepared samples of Niigata sand using three different approaches: air pluviation (PA), air pluviation, and then subjected to a small-strain seismic history (SH), and air pluviation and then subjected to an overconsolidation history (OC). However, in addition to varying the sample preparation technique, Tokimatsu and Uchida (1990) also varied the D_r of the samples, but the intrinsic soil properties of the soil used and all other soil state variables of the samples were held constant. The D_r of the samples ranged from 48% to

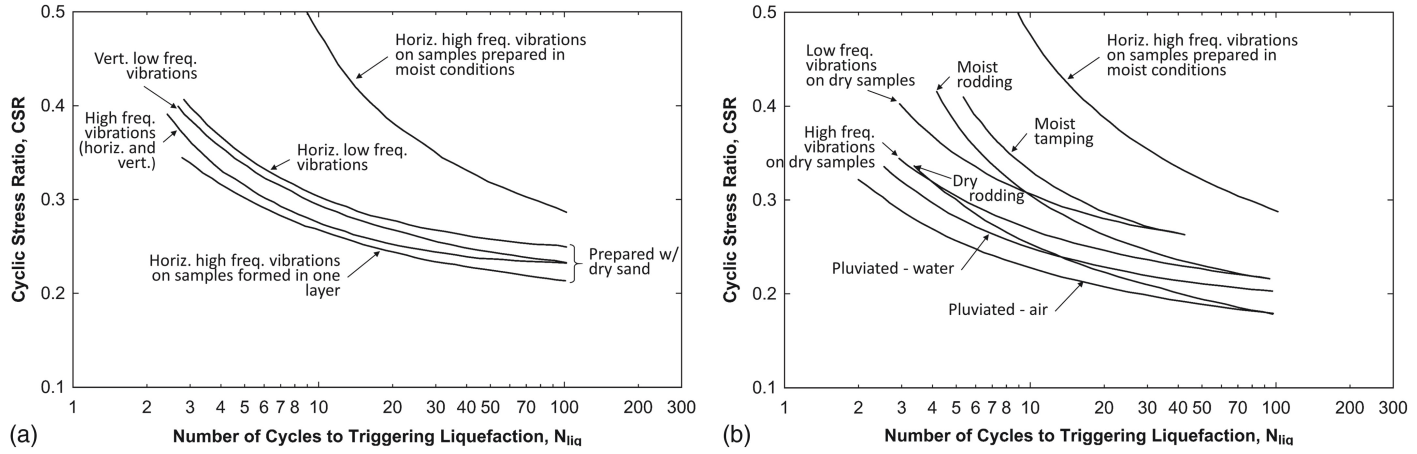

Fig. 1. Cyclic resistance to liquefaction for Monterey No. 0 Sand, $D_r = 50\%$, $\sigma_o' \approx 55$ kPa with samples prepared using several different techniques: (a) vibratory compaction procedures; and (b) compaction procedures. (Adapted from Mulilis et al. 1977.)

J. Geotech. Geoenviron. Eng., 2022, 148(7): 04022056

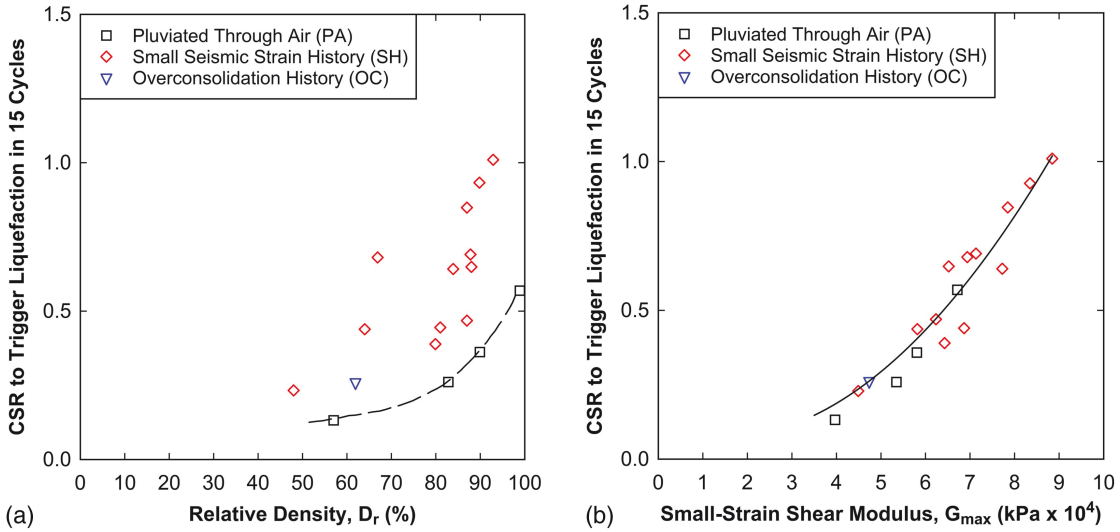

Fig. 2. Influence of sample preparation technique on cyclic resistance to liquefaction of Niigata sand, $\sigma_o' = 98$ kPa, when samples are characterized in terms of (a) D_r; and (b) $G_{\max}$. (Data from Tokimatsu and Uchida 1990.)

100%, and the samples were confined at an initial isotropic effective stress of 98 kPa (~1 atm). The samples were subjected to stress-controlled cyclic triaxial loading, with liquefaction triggering defined as the occurrence of a double-amplitude axial strain of 5%. As shown in Fig. 2(a), the relationship between cyclic resistance to liquefaction and D_r is dependent on the method used to prepare the samples. However, in addition to D_r, Tokimatsu and Uchida (1990) also measured the stiffness of the samples. And, as shown in Fig. 2(b), there is a very strong correlation between the cyclic resistance to liquefaction and $G_{\max}$ of the sand that is independent of sample preparation technique.

As significant as the correlation shown in Fig. 2(b) is, and it is significant, the correlation between the cyclic resistance to liquefaction of a soil and the soil's stiffness is strongly dependent on the intrinsic properties of the soil (e.g., Verdugo 2016). This is illustrated in Fig. 3, which shows the correlation between the cyclic resistance to liquefaction and small-strain stiffness of the soil for different sands and silts. Fig. 3(a) shows cyclic triaxial test data for Niigata and Toyoura sands prepared using the same three techniques used by Tokimatsu and Uchida (1990): PA, SH, and OC (Tokimatsu et al. 1986). While there is a very strong correlation between $G_{\max}$ and cyclic resistance to liquefaction, regardless of the sample preparation technique used, the correlations are unique for each sand due to differences in the intrinsic properties of the sands. Similar trends are shown in Fig. 3(b) for cyclic triaxial test data for two different nonplastic Providence, Rhode Island, silts (Baxter et al. 2008). In this case, the stiffnesses of the silts are quantified in terms of V_S and liquefaction was defined as pore water pressure equaling the initial effective confining stress. [Note: V_S and $G_{\max}$ are both metrics of shear stiffness and are related through

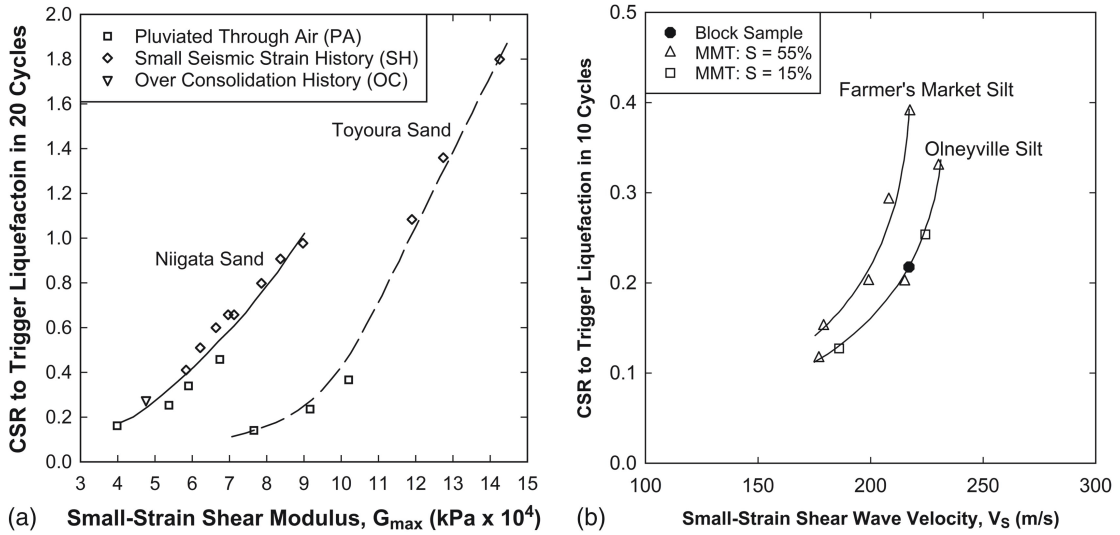

Fig. 3. Correlation between cyclic resistance to liquefaction and small-strain stiffness of soil: (a) Niigata and Toyoura sands with soil stiffness quantified in terms of $G_{\max}$ for samples prepared using three different techniques, $\sigma_o' = 98$ kPa (data from Tokimatsu et al. 1986); and (b) two nonplastic Providence, Rhode Island, silts for undisturbed block samples and reconstituted samples prepared using the modified moist tamping method using two different initial degrees of saturation with soil stiffness quantified in terms of V_S, $\sigma_o' = 100$ kPa (data from Baxter et al. 2008).

the mass density (ρ_t) of the soil: $G_{max} = \rho_t \cdot V_S^2$.] The silt samples were either carved from block samples or reconstituted using a Modified Moist Tamping (MMT) technique proposed by Bradshaw and Baxter (2007) using two different initial degrees of saturation (S). As shown in this figure, while there is a strong correlation between the cyclic resistance to liquefaction and V_S for a given silt that is independent of the sample preparation method, the correlation is unique for each silt due to differences the intrinsic properties of the silts.

These trends are not altogether surprising because V_S and G_{max} are functions of the soil's void ratio (e) (e.g., Hardin and Richart 1963; Richart et al. 1970), not a function of the soil's D_r per se (Alarcon-Guzman et al. 1989). However, the contractive/dilative tendencies of a soil at intermediate strains, which controls liquefaction response of the soil at a given initial stress state, is more influenced by D_r than it is by void ratio (e.g., Seed 1979; Polito and Martin 2003). While D_r and void ratio for a given soil are directly related, one can have different soils that have the same void ratio and initial stress state, and hence have approximately the same G_{max} or V_S, but that have vastly different D_r, and thus, have vastly different cyclic resistances to liquefaction. In short, both D_r and G_{max} (or V_S) are influential parameters on liquefaction triggering, and as discussed subsequently in this paper, this fact is integral to the proposed K_γ factor.

The initial stress state of a soil also has significant influence on the cyclic resistance to liquefaction of the soil. Seed and Lee (1966) is one of the earliest laboratory studies to systematically examine this. Towards this end, they applied the same cyclic shear stress, τ ($= \sigma_d/2$, where σ_d is the deviatoric stress in triaxial loading), to three sets of Sacramento River sand samples prepared using the same technique and to the same D_r, but confined at different initial isotropic effective confining stresses, σ'_o: 50, 75, and 100 kPa (or 0.5, 0.75, and 1.0 atm). They found that the higher the σ'_o, the greater was the number of stress cycles required to trigger liquefaction, where liquefaction was defined both in terms of excess pore water pressures and deformations. They state that this trend was of special interest because it seemingly contradicted what was expected based on critical state theory (i.e., soil having a given D_r becomes more contractive as effective confining stress increases and thus, expectedly, less resistant to liquefaction triggering). However, in their follow-up study, Lee and Seed (1967) empirically observed the resistance to liquefaction increased approximately linearly with σ'_o, implying that τ should be normalized by σ'_o (Seed and Peacock 1971; Finn et al. 1971), where again, liquefaction was defined both in terms of excess pore water pressures and deformations. τ/σ'_o is now widely referred to as Cyclic Stress Ratio (CSR), and the CSR required to trigger liquefaction in a specified number of cycles (e.g., 15 cycles) is now widely referred to as Cyclic Resistance Ratio (CRR). Expressing the cyclic resistance to liquefaction of the soil in terms of τ/σ'_o likely seemed natural because a similar normalization had long been used to express the monotonic undrained shear strength of saturated clays, but for very different reasons (e.g., Green and Marcuson 2014).

Additional laboratory studies (e.g., Seed et al. 1973) showed, however, that the increase in cyclic resistance to liquefaction did not exactly linearly increase with increasing σ'_o, resulting in the introduction of an additional normalization factor, K_σ, which Seed (1983) defined as

$$K_\sigma = \frac{CSR_{\sigma'_o}}{CSR_{\sigma'_o=1\,atm}} \left(or = \frac{CSR_{\sigma'_{vo}}}{CSR_{\sigma'_{vo}=1\,atm}} \right) \quad (1)$$

where $CSR_{\sigma'_o}$ and $CSR_{\sigma'_o=1\,atm} = CSR$ required to trigger liquefaction in a given number of cycles (e.g., 15) in similar samples confined at an initial effective stress of σ'_o and at ~100 kPa (1 atm), respectively. Also, while $CSR_{\sigma'_o}$ and $CSR_{\sigma'_o=1\,atm}$ are appropriate for representing the loading imposed on isotropically consolidated cyclic triaxial samples, $CSR_{\sigma'_{vo}}$ and $CSR_{\sigma'_{vo}=1\,atm}$ are used to represent the loading imposed on soil in-situ where σ'_{vo} is the initial vertical effective stress acting on the soil at a given depth. The slight deviation from linearity in the cyclic resistance to liquefaction is shown in Fig. 4(a) and the corresponding range of K_σ values are shown in Fig. 4(b). [Note that the $K_{2,max}$ values listed in Fig. 4(a) for the different sands relate to G_{max} of the soil, and their relevance will become apparent subsequently in this paper.]

Multiple subsequent laboratory studies have been performed to determine K_σ for various soils, often in support of the seismic design and/or analysis of large earthen dams. Fig. 5 is a plot of K_σ values compiled from literature, and as may be observed from this figure, the scatter in the K_σ values is very large.

Strain-Based Studies

Early studies showed that volumetric strain in a given soil subjected to a given number of loading cycles under drained conditions almost uniquely correlates to the amplitude of the applied cyclic

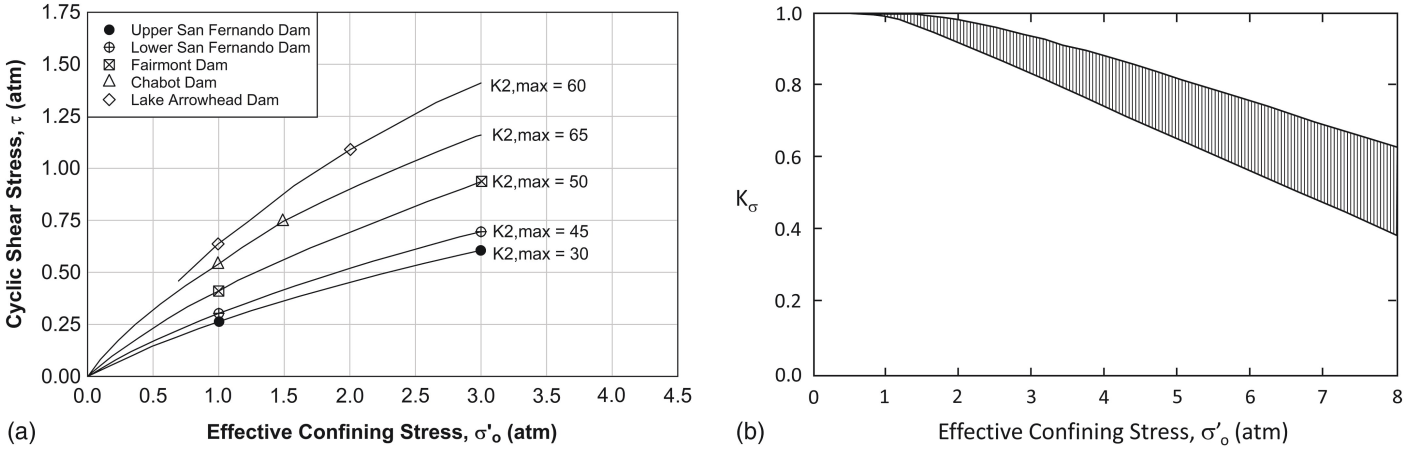

Fig. 4. (a) Cyclic shear stress, τ, to trigger liquefaction in 10 cycles of cyclic triaxial loading in different sands versus σ'_o; and (b) K_σ relationship based on data from (a), among other data. (Adapted from Seed 1983.)

J. Geotech. Geoenviron. Eng., 2022, 148(7): 04022056

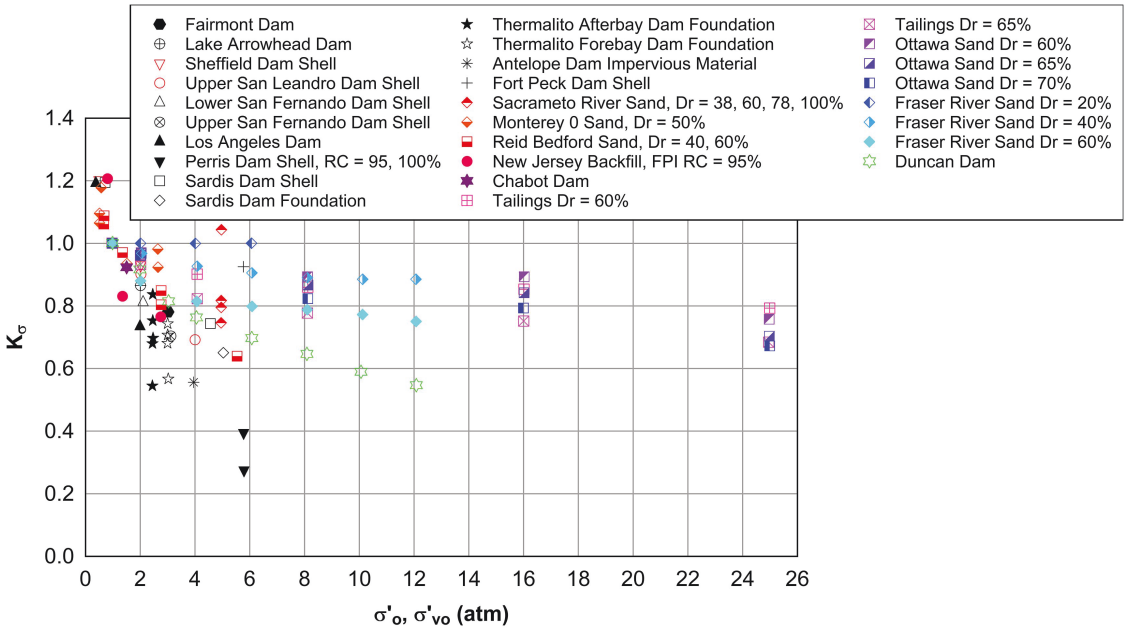

Fig. 5. K_σ data compiled from literature. (Data from Seed and Harder 1989; Pillai and Byrne 1994.)

shear strain, γ, rather than the applied τ (or CSR) (e.g., Silver and Seed 1971). The corollary of this finding is that the excess pore pressure ratio (r_u: $r_u = \Delta u/\sigma'_{vo}$, where Δu is the excess pore water pressure) in a given saturated soil subjected to cyclic loading under undrained conditions almost uniquely correlates to the amplitude of the applied γ, rather than the applied τ (or CSR) (e.g., Martin et al. 1975). In line with these findings, Dobry et al. (1982) proposed a strain-based approach for evaluating liquefaction triggering as an alternative to the stress-based approach. The procedure entails quantifying the amplitude of the ground shaking in terms of γ and the duration of the shaking in terms of number of equivalent strain cycles ($n_{eq\gamma}$) and correlating these to r_u, where $r_u \approx 1$ signifies liquefaction triggering.

As shown in Fig. 6, one very attractive attribute of quantifying loading in terms of γ and $n_{eq\gamma}$ is that their relationship to r_u is relatively independent of the intrinsic properties of the soil and soil state variables. In this figure, r_u is shown as a function of γ and $n_{eq\gamma} = 10$ for different soil samples having a range of intrinsic soil properties and soil state variables. And, while there is some scatter in the data, the correlation is very strong. However, as detailed in Rodriguez-Arriaga and Green (2018) and Green and Rodriguez-Arriaga (2019), the shortfall of the procedure is correlating γ and $n_{eq\gamma}$ to earthquake ground motions parameters. In contrast to correlating τ (or CSR) and number of equivalent stress cycles ($n_{eq\tau}$) to the amplitude and duration of earthquake ground motions, respectively, which can be done within a total stress framework, correlations with γ and $n_{eq\gamma}$ need to be done within an effective stress framework. The difference between the two frameworks is that influence of excess pore water pressure generation on soil response needs to be explicitly accounted for in an effective stress framework but does not within a total stress framework. [Note: The differences in the frameworks is the same for quantifying the monotonic shear strength of a soil as it is for quantifying the cyclic resistance to liquefaction, e.g., Green and Marcuson (2014).]

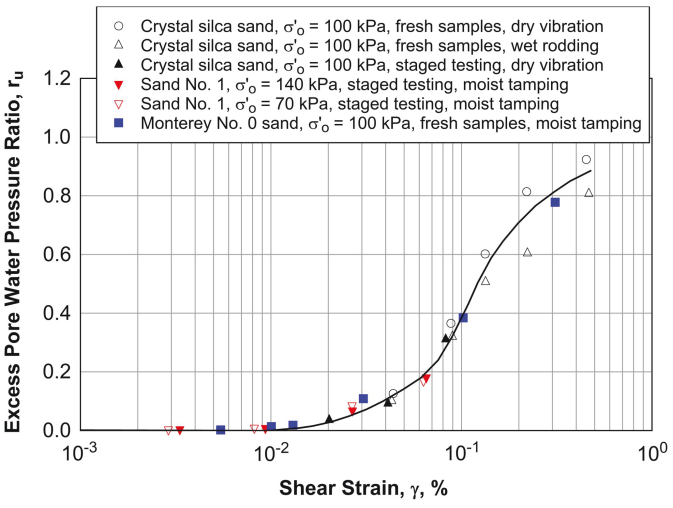

Fig. 6. Excess pore water pressure ratio, r_u, for different sands having D_r of 60% after 10 cycles of strain-controlled triaxial loading. (Data from Dobry et al. 1982.)

Cyclic shear stress, τ (or CSR) is related to the peak horizontal ground acceleration (a_{max}) of the ground motions within a total stress framework using Newton's second law (e.g., Whitman 1971; Seed and Idriss 1971) in conjunction with a phenomenological factor r_d that accounts for the non-rigid response of the profile (e.g., Seed and Idriss 1971; Lasley et al. 2016). However, to relate τ to γ, the nonlinear response of the soil to cyclic loading, to include the softening of the soil due to decreases in effective confining stress resulting from the excess pore water pressure generation as shaking progresses, needs to be accounted for. Accounting for these effects is extremely complex and inherently needs to be performed within an effective stress framework. The need for total stress versus effective stress frameworks also applies to computing number of equivalent stress cycles and number of equivalent strain cycles, $n_{eq\tau}$, versus $n_{eq\gamma}$. In short, when the loading is quantified in terms of τ (or CSR) and $n_{eq\tau}$, the excess pore water response of the soil and its influence on soil stiffness are not known; however, it is not necessary to know either of these

because the cyclic resistance to liquefaction of the soil is quantified in terms of τ (or CRR) as a function of $n_{eq\tau}$. This is not the case when the loading and cyclic resistance to liquefaction is quantified in terms of γ and $n_{eq\gamma}$. Aside from the issues related to implementation of the Dobry et al. (1982) strain-based procedure for evaluating liquefaction triggering, the correlation between γ and $n_{eq\gamma}$ to r_u is very significant and is integral to the proposed K_γ factor, as discussed next.

Conceptual Basis for the K_γ Factor

The findings from Dobry et al. (1982) that there is a unique relationship between γ and $n_{eq\gamma}$, and excess pore water pressure generation for a wide range of soils can be used to explain the trends observed by Seed and Lee (1966) and Seed (1983) on the influence of initial stress state on liquefaction triggering. Conceptually this is shown in Fig. 7 using τ-γ curves modeled by the shear modulus reduction curve relationship proposed by Ishibashi and Zhang (1993) [IZ93] for cohesionless soil (i.e., Plasticity Index, PI, equal to zero). The IZ93 curves correlate the ratio of the secant shear modulus, G, and $G_{\max}$ as a function of γ (i.e., $G/G_{\max}$ versus γ), and the τ-γ curves can be obtained from the IZ93 modulus reduction curves if $G_{\max}$ of the soil is known: $\tau = G_{\max} \cdot (G/G_{\max}) \cdot \gamma$. The IZ93 curves are empirically based, derived from numerous tests performed on multiple soils having a range of intrinsic soil properties and soil state variables.

Fig. 7(a) shows that when a given amplitude τ is imposed on similar soil samples confined at different effective stresses, the shear strain induced in the sample confined at the higher confining stress (e.g., ~500 kPa or 5 atm) is much less than that induced in the sample confined at ~100 kPa (1 atm) (i.e., $\gamma_\sigma < \gamma_1$). As a result, the sample confined at the higher confining stress would require more cycles of loading to liquefy (i.e., an apparent higher resistance to liquefaction, despite having higher contractive tendencies at larger strains commensurate with critical state), which is consistent with observations made by Seed and Lee (1966). However, when the amplitude of the load quantified in terms of CSR is imposed on the two samples [Fig. 7(b)], the shear strain induced in the sample confined at the higher confining stress (e.g., ~500 kPa or 5 atm) is slightly greater than that induced in the sample confined at ~100 kPa (1 atm) (i.e., $\gamma_\sigma > \gamma_1$). As a result, the sample confined at the higher confining stress would require slightly fewer cycles of loading to liquefy (e.g., Seed et al. 1973; Seed 1983). Hence, the additional need to normalize CSR by K_σ is so that when the loading is quantified in terms of CSR/K_σ, $\gamma_\sigma \approx \gamma_1$, and thus, both samples liquefy in approximately the same number of cycles [Fig. 7(c)].

As may be noted, only the first quarter cycle of loading is shown in Fig. 7. This is because, if during the first quarter cycle of loading, the induced shear strain is the same in the two samples confined at

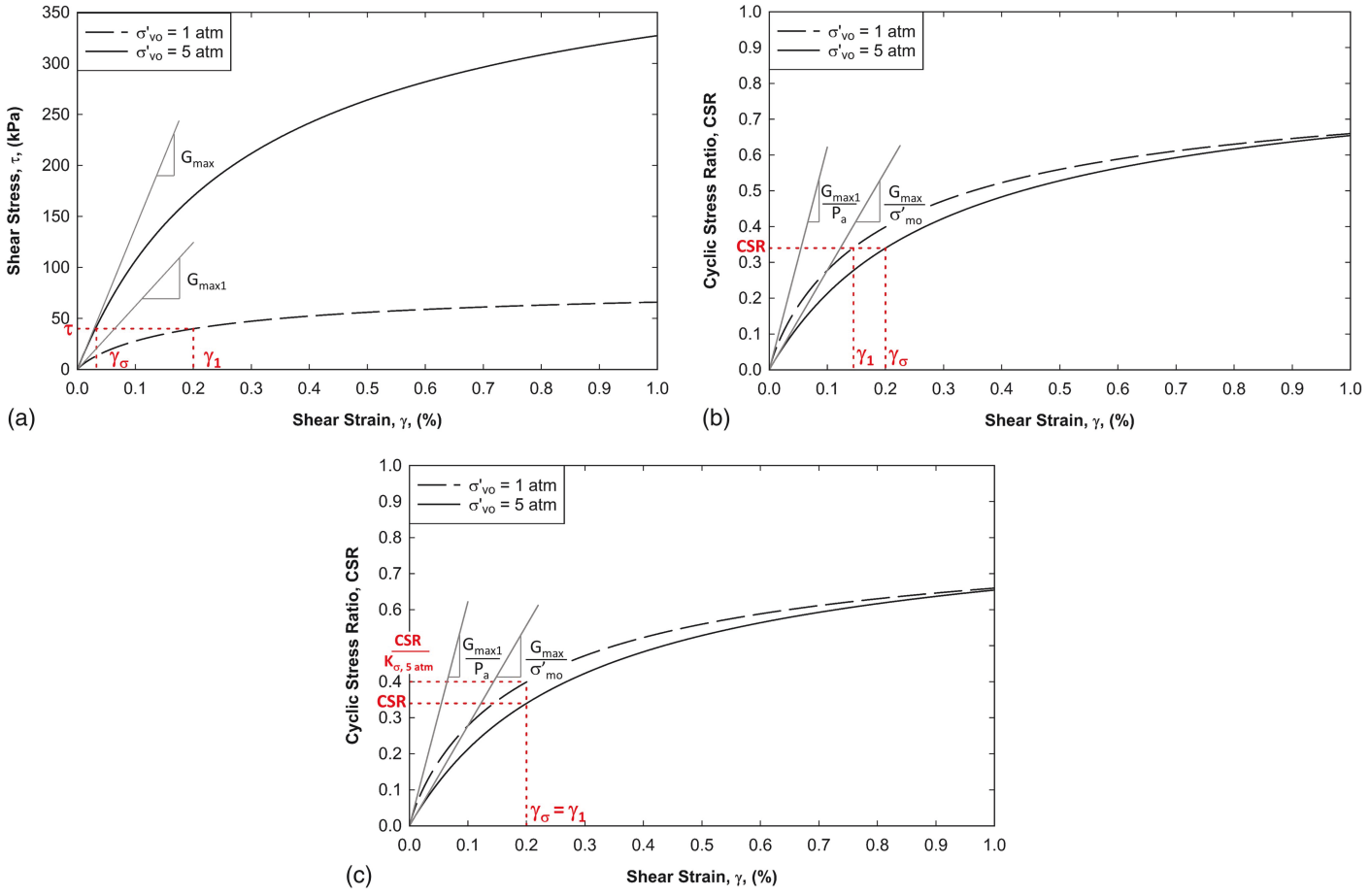

Fig. 7. Shear stress–shear strain (τ-γ) response of soil for various conditions: (a) soil having same density, but confined at different σ'_{vo} and subjected to cyclic loading of amplitude τ; (b) same conditions as described in (a) but the amplitude of the cyclic loading is quantified in terms of CSR (i.e., τ/σ'_{vo}); and (c) same conditions as described in (a and b) but the amplitude of the cyclic loading is quantified in terms of CSR/K_σ (or CSR/K_γ).

J. Geotech. Geoenviron. Eng., 2022, 148(7): 04022056

different σ'_{vo} and loaded to different *CSRs* (all else being equal), then the incremental increase in excess pore water pressure ratio will be the same (Fig. 6) and the resulting degradation of the soil stiffness will be the same (Martin et al. 1975; Byrne 1991). As a result, during subsequent load increments, the induced strains in the two samples will again be the same, the incremental increase excess pore water pressure ratio will be the same, and thus the degradation in stiffness of the samples will again be the same. This trend progresses with each load increment until liquefaction is triggered, regardless of how liquefaction is defined. This progression differs from the Dobry et al. (1982) strain-based procedure where the degradation in soil stiffness due to excess pore water pressure generation needs to be known for each load increment in order to relate the applied τ (or *CSR*) to the induced γ, which requires an effective stress framework for the analysis (Rodriguez-Arriaga and Green 2018; Green and Rodriguez-Arriaga 2019).

The concept of normalizing τ by σ'_{vo} and the further normalization by K_σ such that the resulting γ induced in a soil confined at the reference condition of $\sigma'_{vo} \approx 100$ kPa (1 atm) is equal to that induced in the same soil confined at σ'_{vo} forms the basis for the proposed K_γ factor. Note: To distinguish the proposed approach from past, largely empirically based approaches, hence forth, the "K_σ values" computed by equating induced shear strains per the approach proposed herein are referred to as K_γ [i.e., computed per Fig. 7(c)], while K_σ is reserved for values computed per Eq. (1) from cyclic laboratory test data.

A flow chart on how K_γ is computed in presented in Fig. 8, which entails an iterative approach for determining shear strain induced in a soil initially confined to a vertical effective stress of σ'_{vo}, a lateral effective stress of $K_o \cdot \sigma'_{vo}$, and subject to a loading τ ($=CSR \cdot \sigma'_{vo}$), where K_o is the at-rest lateral earth pressure coefficient. The iteration is performed using a modulus reduction curve (e.g., Ishibashi and Zhang 1993) scaled to the $G_{\max}$ of the soil and the initial mean effective confining stress, σ'_{mo}; the iterative process is similar to the procedure incorporated in equivalent linear site response software. Once the induced shear strain, γ, is determined, K_γ is computed as the ratio of the *CSR* imposed on the soil in its actual initial conditions and the *CSR* required to induce the same γ in the soil if it were confined at a vertical effective stress of $\sigma'_v \approx 100$ kPa (1 atm) and a lateral effective stress of $K_o \cdot \sigma'_v$ (i.e., CSR_1): $K_\gamma = CSR/CSR_1$. The modulus reduction curve scaled to $G_{\max 1}$ and σ'_{mo} corresponding to $\sigma'_v \approx 100$ kPa (1 atm) is used to determine shear stress (τ_1) corresponding to the induced γ, and $CSR_1 = \tau_1/P_a$, where P_a is the atmospheric pressure in the same units as τ_1. [Note: $G_{\max 1}$ is $G_{\max}$ normalized to $\sigma'_o \approx 100$ kPa (1 atm).] Conceptually, this is the same approach illustrated in Fig. 7(c) and is used to compute the K_γ values subsequently.

Alternative to using the approach shown in Fig. 8, approximate values of K_γ can be computed using the equations detailed in the Supplemental Materials. These equations were derived such that they yield similar K_γ values to those obtained following the flow chart in Fig. 8, but without the need to iterate using the modulus reduction curves. Also, as may be noted in Fig. 8 and the approximate equations presented in the Supplemental Materials, K_γ is limited to a maximum value of 1.3, where this upper limit is based on judgement, similar to the limit imposed on K_σ by Youd et al. (2001), i.e., $K_\sigma \leq 1$, and by Idriss and Boulanger (2008), i.e., $K_\sigma \leq 1.1$. Higher values of K_γ may be used once tests are preformed to validate the proposed approach for very low confining stresses (i.e., confining stresses that result in $K_\gamma > 1.3$).

The concept of equating the induced γ to compute K_γ in two samples is explored further in the next section using several laboratory test datasets from literature.

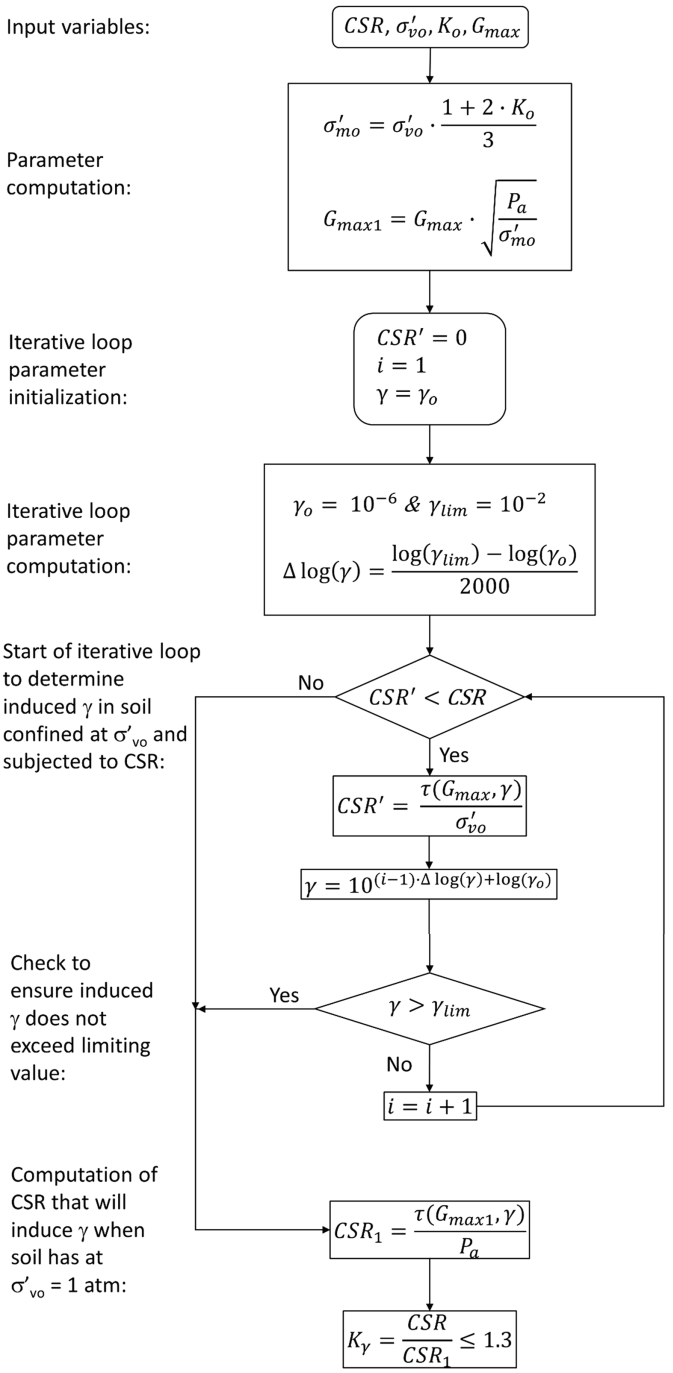

Fig. 8. Flow chart for computing K_γ using modulus reduction curves.

Validation of the K_γ Concept

Direct Validation

The data in Fig. 4(a) from Seed (1983) are analyzed where K_γ is determined following the approach illustrated in Figs. 7(c) and 8 [i.e., determining the value of K_γ such that the when CSR/K_γ and *CSR* are imposed on the same soil confined at σ'_{vo} and $\sigma'_{vo} \approx 100$ kPa (1 atm), respectively, the resulting strains are equal]. To this end, the IZ93 shear modulus reduction curve relationship for cohesionless soil is again used to model the τ–γ behavior of the soil. In order to compute τ versus γ, $G_{\max}$ of the soil is needed [i.e., $\tau = G_{\max} \cdot (G/G_{\max}) \cdot \gamma$], and it can be calculated directly

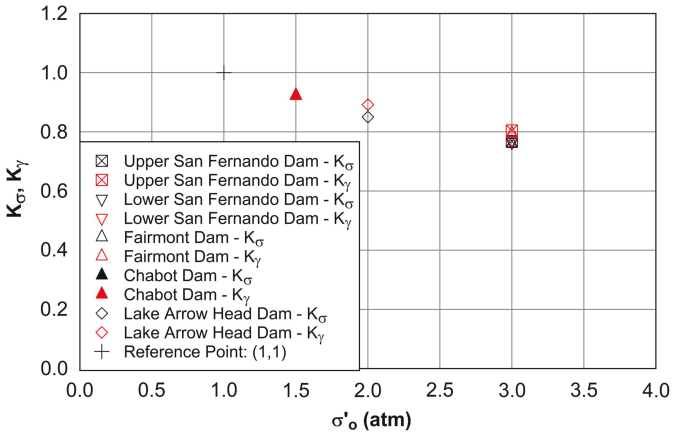

Fig. 9. K_σ values computed from laboratory data from Seed (1983) and per the approach illustrated in Figs. 7(c) and 8 (i.e., K_γ). [Note that data for other soils are presented in Seed 1983, but these other soils were not tested for $\sigma'_o \approx 100$ kPa (1 atm), which is needed to compute K_σ per Eq. (1); thus, these additional data are not included herein.]

from the Seed (1983) data in Fig. 4(a) using the $K_{2,\max}$ values (Seed and Idriss 1970)

$$G_{\max} = 22.36 \cdot P_{a1} \cdot K_{2,\max} \cdot \sqrt{\frac{\sigma'_{mo}}{P_{a2}}} \tag{2}$$

where P_{a1} and P_{a2} = atmospheric pressure in the same units as $G_{\max}$ and σ'_{mo}, respectively; and as can be surmised from Eq. (2), $K_{2,\max}$ is simply $G_{\max}$ normalized for mean effective confining stress. Values of K_γ computed using the flow chart in Fig. 8 are compared to the laboratory-determined K_σ values, and the agreement is excellent (Fig. 9).

To further assess the validity of the K_γ-concept, cyclic triaxial test data for several sands presented in Tokimatsu and Uchida (1990) are analyzed, to include those previously shown in Fig. 2, where the samples were characterized in terms of G_{max}, as well as D_r, and the tests were performed at different σ'_o. Much more data are provided in Tokimatsu and Uchida (1990) for Niigata and Toyoura sands than the other sands they tested, and thus, only Niigata and Toyoura sands are analyzed herein. Unfortunately, even for Niigata and Toyoura sands, data for only a few tests are presented for conditions where σ'_o is other than 100 kPa (~1 atm), precluding an accurate determination of K_σ directly from the laboratory test data. However, K_γ values can be computed for each individual test per the approach illustrated in Figs. 7(c) and 8, and plots of CSR versus $G_{\max 1}$ and CSR/K_γ versus $G_{\max 1}$ are compared to see if the normalization of CSR by K_γ results in the data plotting in what can be described as a "narrower band." The results are shown in Figs. 10(a and b) for the Niigata and Toyoura sands, respectively. Although there is scatter in the data and only a limited number of tests were performed for $\sigma'_o \neq 100$ kPa, the normalization of CSR by K_γ does result in the data plotting in a narrower band for both sands (i.e., the filled circles and filled triangles are more in line with the open squares than the open circles and open triangles are).

Interestingly, Tokimatsu and Uchida (1990) noted that the data plotted in a slightly narrower band when CSR was plotted as function of $G_{\max 1^*}$, instead of CSR versus $G_{\max 1}$; $G_{\max 1^*}$ is defined as

$$G_{\max 1^*} = G_{\max} \cdot \left(\frac{P_a}{\sigma'_{mo}}\right)^m \tag{3}$$

where P_a = atmospheric pressure in the same units as σ'_{mo}; and $G_{\max}$ and $G_{\max 1^*}$ have the same units; and m is 2/3, instead of the standard value of 1/2 used to compute $G_{\max 1}$ (e.g., Hardin and Richart 1963; Richart et al. 1970). Tokimatsu and Uchida (1990, p. 37) state: "The possible cause of this unexpected result is the effects of confining pressure on the stress ratio causing liquefaction," but they did not pursue the issue further. Their observation is, in fact, the "other side of the coin" to normalizing CSR by K_γ determined per Figs. 7(c) and 8. The IZ93 curves were used to compute test-specific m values for the Niigata and Toyoura sand data such that $\gamma_\sigma = \gamma_1$ for each test. The resulting m values varied from 0.505 to 0.605 for the Niigata sand tests and from 0.543 to 0.651 for the Toyoura sand tests, not too different from the value of $m = 2/3$ determined by simple visual observation by Tokimatsu and Uchida (1990).

A similar exercise to that presented in the preceding paragraph for the Niigata and Toyoura sands was performed using the cyclic triaxial data for silty fine sand presented in Wang et al. (2006), wherein the samples were characterized using V_S. Although not shown due to space limitations, the resulting trends are identical

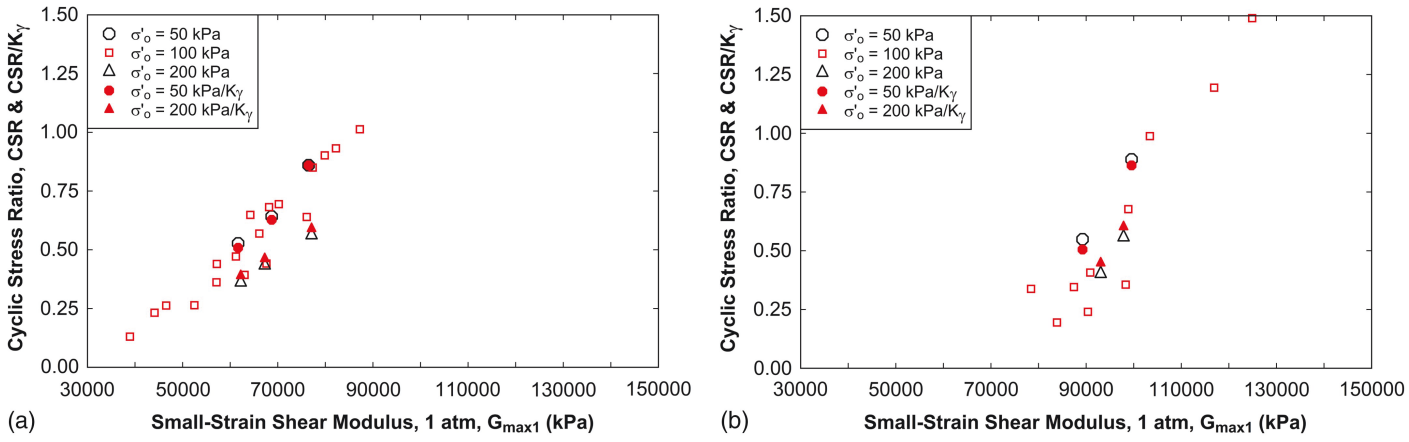

Fig. 10. Stress-controlled cyclic triaxial test data for Niigata and Toyoura sands: (a) Niigata sand—CSR versus $G_{\max 1}$ and CSR/K_γ versus $G_{\max 1}$; and (b) Toyoura sand—CSR versus $G_{\max 1}$ and CSR/K_γ versus $G_{\max 1}$. Of significance in these plots is that the filled circles and triangles are more in line with the open squares than the open circles and triangles are. (Data from Tokimatsu and Uchida 1990.)

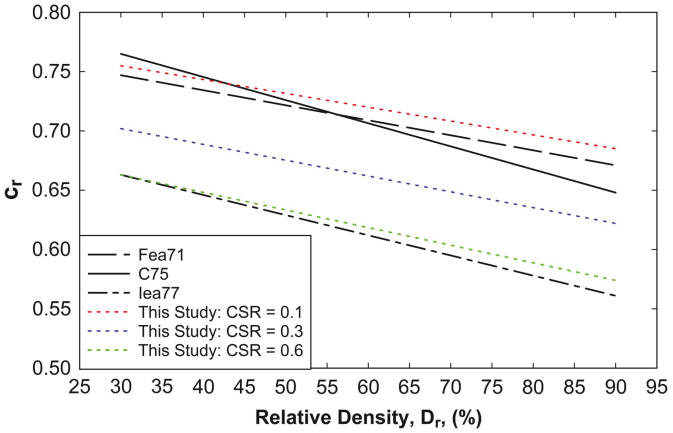

Fig. 11. c_r values computed using Eqs. (5) and (6).

to those presented above for the Niigata and Toyoura sands, further validating the K_γ-concept.

Influence of Lateral Effective Confining Stress (c_r) Using the K_γ-Concept

In the preceding section, the influence of the initial vertical effective confining stress on liquefaction triggering is analyzed. However, the concept of normalizing *CSR* such that the γ induced in a soil confined under a given set of conditions should be equal to the γ induced in the same soil confined under a reference set of conditions is more general than applying just to soils confined under different values of σ'_{vo} (i.e., K_σ). Several studies have investigated the influence of lateral earth pressure on liquefaction triggering, particularly with a focus on relating cyclic triaxial test results where the samples are isotropically consolidated to anisotropically consolidated conditions. These studies include Finn et al. (1971) [Fea71], Castro (1975) [C75], and Ishihara et al. (1977) [Iea77], among others. The factor accounting for isotropic versus anisotropic consolidation has been designated as c_r

$$CSR_{ss} = c_r \cdot CSR_{tx} \tag{4}$$

where CSR_{ss} = the *CSR* required to trigger liquefaction in a given soil anisotropically consolidated under at-rest conditions in a given number of cycles of cyclic simple shear or torsional shear loading; and CSR_{tx} = the *CSR* required to trigger liquefaction in an isotropically consolidated sample of the same soil in the same number of cycles in a cyclic triaxial apparatus. Proposed relationships for c_r include

$$c_r = \frac{1 + K_o}{2} \text{ (Finn et al. 1971)} \tag{5a}$$

$$c_r = \frac{2 \cdot (1 + K_o)}{3\sqrt{3}} \text{ (Castro 1975)} \tag{5b}$$

$$c_r = \frac{1 + 2 \cdot K_o}{3} \text{ (Ishihara et al. 1977)} \tag{5c}$$

Plots of the c_r relationships are shown in Fig. 11 for a range of D_r, where the at-rest lateral earth pressure coefficient (K_o) is estimated as

$$K_o = 1 - \sin(\phi') \tag{6a}$$

where ϕ' = angle of internal friction, which is estimated as

$$\phi' = 25 + 0.18 \cdot D_r(\%) \tag{6b}$$

Also shown in Fig. 11 are the c_r values computed by equating the induced shear strains in the isotropically and anisotropically consolidated soils, for $CSR = 0.1$, 0.3, and 0.6. The τ-γ curves were modeled using IZ93 and $G_{\max}$ was computed using the relationship proposed by Richart et al. (1970) for "round-grained" sands:

$$G_{\max} = 686 \cdot P_{a1} \frac{(2.17 - e)^2}{1 + e} \left(\frac{\sigma'_{mo}}{P_{a2}}\right)^{0.5} \tag{7}$$

where e = void ratio; $G_{\max}$ and P_{a1} have the same units; and σ'_{mo} and P_{a2} have the same units. To relate void ratio to D_r, the minimum and maximum void ratios for Ottawa sand were used (i.e., $e_{\max} = 0.8$ and $e_{\min} = 0.5$), where Ottawa sand was used in the development of the c_r relationships proposed by Finn et al. (1971) and Castro (1975). As may be observed from Fig. 11, the c_r relationship computed by equating induced shear strains have approximately the same sensitivity to D_r as the other relationships and covers the same range as the other proposed relationships.

To assess the efficacy of the different c_r relationships, triaxial cyclic torsional shear test data from Ishihara et al. (1977) are analyzed. The data are for Fuji River sand, which is a uniform fine sand having $e_{\max} = 1.03$ and $e_{\min} = 0.48$. All samples tested had a $D_r \approx 55\%$, $\sigma'_{vo} = 98.1$ kPa (~1 atm), and $K_o = 0.5$, 1.0, or 1.5, and liquefaction was defined as excess pore water pressure equaling σ'_{vo} (i.e., $r_u = 1.0$). The test results are shown in Fig. 12(a), and the cyclic resistance to liquefaction of the soil increases as lateral stress increases. This is expected because σ'_{mo} increases as lateral stress increases, and the small-strain shear modulus ($G_{\max}$) of the soil is proportional to the square root of σ'_{mo} (e.g., Hardin and Richart 1963; Richart et al. 1970). This is also consistent within the K_γ-concept. As $G_{\max}$ increases due to an increase in lateral effective stress, the induced strain would decrease for a given *CSR*, thus increasing the apparent cyclic resistance to liquefaction.

To allow a comparison, the *CSR* applied to the samples is normalized by c_r values computed per Eqs. (5) and (6), and the results plotted in Figs. 12(b–d). As may be observed from these plots, all the c_r relationships result in the data plotting in a narrower band, and it is difficult to state which c_r relationship is superior to the others. c_r is also computed by equating the strains induced in a sample having $K_o \neq 1$ and $K_o = 1$. Towards this end, $G_{\max}$ of the soil is estimated using the following relationship (Hardin and Richart 1963) and the τ-γ response of the soil is modeled using IZ93 curves

$$G_{\max} = 485 \cdot P_{a1} \frac{(2.17 - e)^2}{1 + e} \left(\frac{\sigma'_{mo}}{P_{a2}}\right)^{0.5} \tag{8}$$

where $G_{\max}$ and P_{a1} have the same units; and σ'_{mo} and P_{a2} have the same units. As may be noted, Eq. (8) is a slight deviation of Eq. (7), with the deviation based on a relationship relating D_r and V_S used by Yi (2010) to analyze Fuji River sand laboratory data. The triaxial cyclic torsional shear test data were then normalized by the computed c_r values using the K_γ-concept, and the results are shown in Fig. 12(e). Using the K_γ-concept yields comparable results to published c_r values, which provides further credence to the approach and illustrates its broader significance over K_σ.

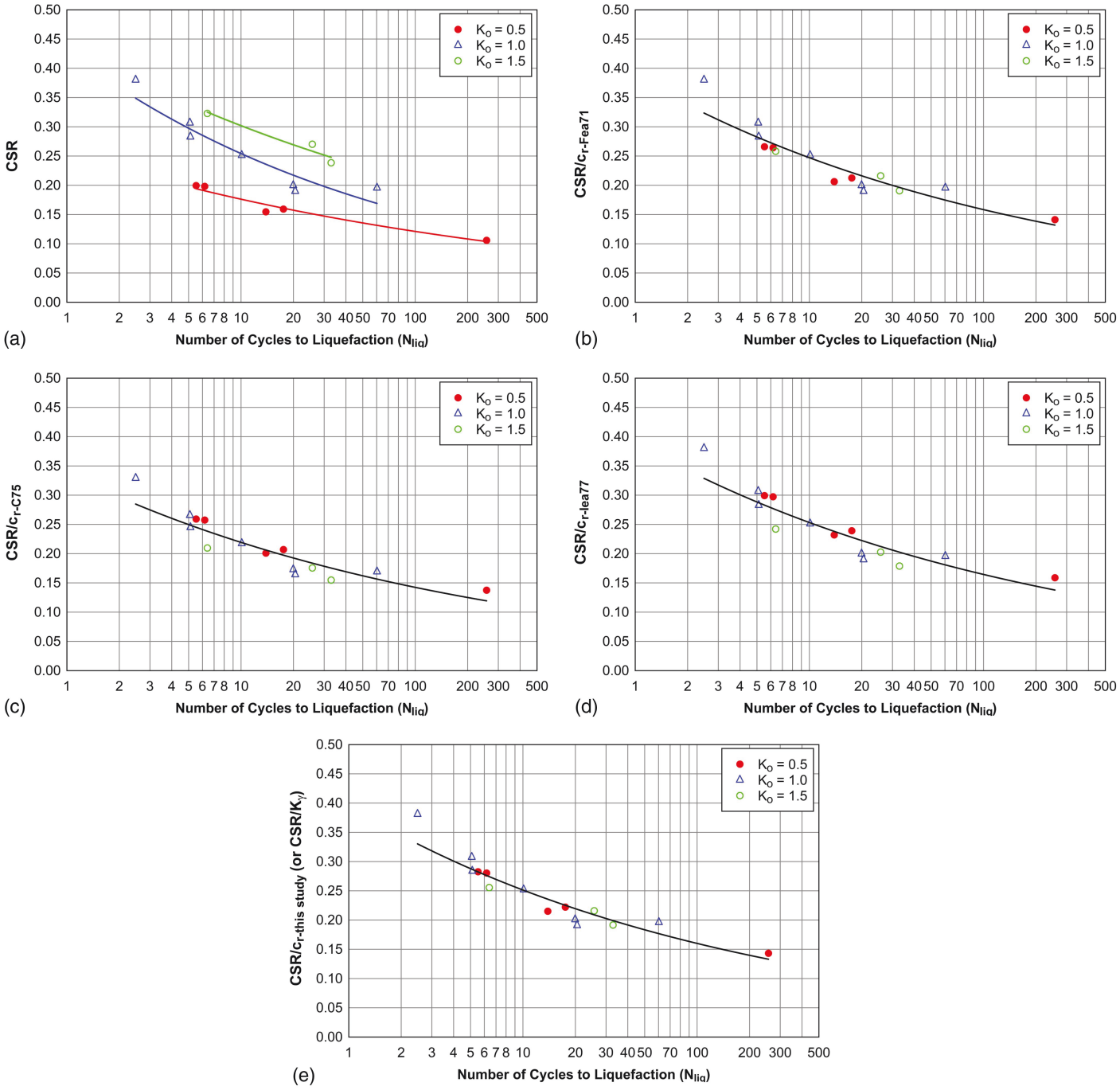

Fig. 12. (a) Stress-controlled triaxial cyclic torsional shear test data for Fuji River sand, $D_r = 55\%$ and $K_o = 0.5$, 1.0, and 1.5 (data from Ishihara et al. 1977); (b) same data as shown in (a) normalized using c_r relationship proposed by Finn et al. (1971), Eq. (5*a*); (c) same data as shown in (a) normalized using c_r relationship proposed by Castro (1975), Eq. (5*b*); (d) same data as shown in (a) normalized using c_r relationship proposed by Ishihara et al. (1977), Eq. (5*c*); and (e) same data as shown in (a) normalized using c_r computed using the approach illustrated in Figs. 7(c) and 8.

Discussion

K_γ versus K_σ

Although the proposed K_γ factor should be used in place of K_σ in the development of future simplified stress-based triggering frameworks, K_σ and K_γ are conceptually very different. Where most previously proposed K_σ relationships have largely been empirically based and only account for the influence of σ'_{vo} on a soil's cyclic resistance to liquefaction, K_γ is more mechanically based and accounts for the influence of a broader range of intrinsic soil properties and soil stress states on liquefaction triggering (e.g., the influence of σ'_{vo}, lateral stress, and soil fabric, among others). Underlying these additional accoutrements of K_γ is that K_γ is a function of the soil stiffness (G_{max} or V_S) and relates to the loading imposed on the soil, not the cyclic resistance of the soil. From a pragmatic perspective K_γ and K_σ are numerically similar for young, normally K_o-consolidated soils when the factor of safety

Table 1. Data from Duncan Dam study

	σ'_{vo} (kPa) [atm]							
	100 [1]	200 [2]	300 [3]	400 [4]	600 [6]	800 [8]	1,000 [10]	1,200 [12]
$N_{1,60cs}$ (blws/30 cm)	10	11	12.4	13.2	14.5	15.7	17.3	18.5
CRR	0.12	0.12	0.12	0.12	0.12	0.12	0.12	0.12
K_σ	1.0	0.92	0.80	0.75	0.70	0.67	0.57	0.54
K_γ	1.0	0.87	0.80	0.76	0.70	0.66	0.63	0.61

Source: Data from Pillai and Byrne (1994).

(FS) against liquefaction is equal to one (i.e., $CSR = CRR$). Some of the differences between K_γ and K_σ are illustrated in the following using data from the detailed and in depth study performed on Duncan Dam in British Columbia, Canada (Pillai and Byrne 1994).

The Pillai and Byrne (1994) study entailed the performance of isotropically consolidated cyclic triaxial tests and cyclic simple shear tests performed on undisturbed samples obtained by frozen sampling of the foundation soils of Duncan Dam. The samples were confined at σ'_o and σ'_{vo} up to 1,200 kPa (~12 atm), corresponding to different depths of interest below the dam. The normalized SPT blow counts ($N_{1,60cs}$) of the in-situ deposit corresponding to these depths are listed in Table 1. Liquefaction was considered to have been initiated when the sample experienced 2.5% and 4.0% single amplitude strain in the cyclic triaxial and cyclic simple shear tests, respectively. The K_σ values for the stresses considered are also listed in Table 1 and are plotted in Fig. 13(a). To compute K_γ, $G_{\max}$ for the samples had to be estimated. To this end, V_S was estimated from $N_{1,60cs}$ using slightly modified version of the equation proposed by Ulmer et al. (2020), Eq. (9). The modification was made by calibrating the V_S-$N_{1,60cs}$ correlation such that the proposed approach for computing K_γ yielded a similar value to the laboratory determined value for K_σ at $\sigma'_{vo} = 600$ kPa (~6 atm), although the K_σ value for any σ'_{vo} could have been used. Again, this modification was slight and results in V_S values that are well within the range of values predicted using $N_{1,60cs}$ via other published correlations (e.g., Wair et al. 2012)

$$V_s = 61.89 \cdot (N_{1,60cs})^{0.4} \cdot \left(\frac{\sigma'_{mo}}{P_a}\right)^{0.25} \tag{9}$$

where V_S is in m/s; $N_{1,60cs}$ is in blows/30 cm; and σ'_{mo} and P_a are in the same units. $G_{\max}$ and V_S were related assuming $\rho_t = 2$ kg/m^3, based on the characteristics of the soil. As may be observed from Fig. 13(a), there is exceptionally good agreement between the K_σ laboratory values and the K_γ values, with the largest errors being for the highest confining stresses, $\sigma'_{vo} = 1{,}000$ and 1,200 kPa (~10 and ~12 atm, respectively), albeit relatively small errors. This comparison serves to give further credence to the K_γ-concept, even though V_S for the samples is estimated and not measured directly. [Note: The K_σ data plotted in Fig. 13(a) are also included in Fig. 5. Accordingly, the comparison of these K_σ values and the computed K_γ values plotted in Fig. 13(a) should be viewed from the perspective of the large scatter in K_σ shown in Fig. 5.]

The dependency of K_γ on CSR is in contrast to the laboratory data-based K_σ relationships that inherently assume $CSR = CRR$ (i.e., FS against liquefaction triggering is equal to one). The significance of this can be seen in Fig. 13(b) wherein the K_γ values corresponding to specific CSR and $N_{1,60cs}$ values are plotted; these are the same K_γ values that are plotted in Fig. 13(a). However, in addition to the K_γ values for specific depths, K_γ curves are computed and plotted for these same CSR and $N_{1,60cs}$ values for a range of overburden pressures. Specific to the K_γ values for Duncan Dam, the $N_{1,60cs}$ increases with each depth, but the CSR values corresponding to a $FS = 1$ are the same (i.e., $CSR = 0.12$) (Pillai and Byrne 1994). However, if we consider, for example, $N_{1,60cs} = 18.5$ blws/30 cm, which is the value of $N_{1,60cs}$ at $\sigma'_{vo} = 1{,}200$ kPa (~12 atm), and $CSR = 0.1$ and 0.4 (i.e., FS > 1 and FS < 1, respectively), the K_γ curves are very different. The reason for this is that the strain induced in the soil is a function of the imposed CSR and that the contractive/dilative tendencies of the soil varies significantly as a function of strain up to critical state.

The FS were computed for $CSR = 0.1$ and 0.4 for a range of σ'_{vo} for two conditions. First, the FS were computed using K_γ values corresponding to $FS = 1$, which is consistent to computing the FS using laboratory derived K_σ values (i.e., $FS_{K\sigma}$). Second, the FS were computed using K_γ values that corresponded to the "actual" FS, per the proposed use of the K_γ relationship (i.e., $FS_{K\gamma}$). Curves of the ratios of these computed FS are shown in Fig. 14

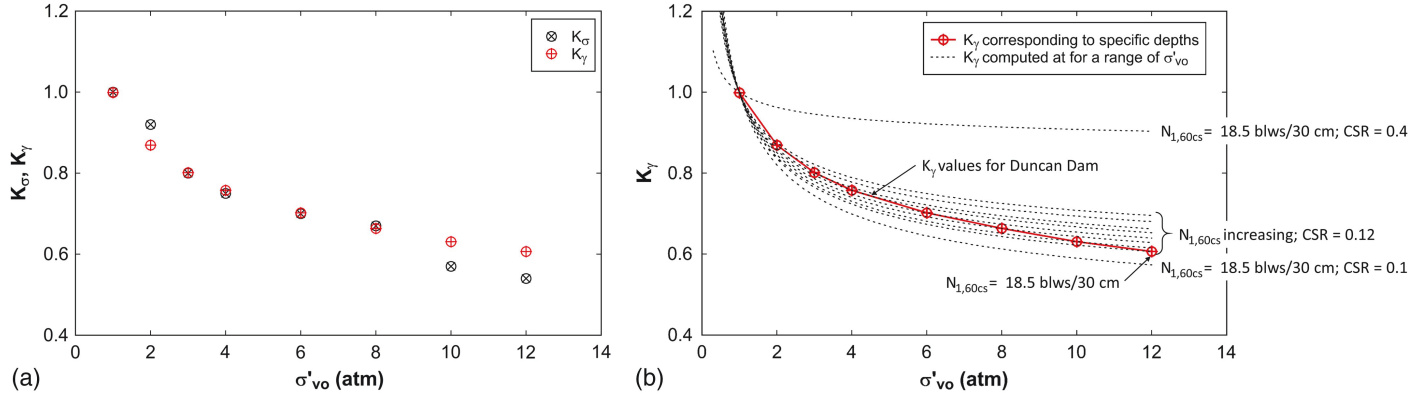

Fig. 13. (a) K_σ values based on laboratory data for undisturbed samples from the foundation sands from Duncan Dam and K_γ values corresponding to specific depths (σ'_{vo} and $N_{1,60cs}$) (data from Pillai and Byrne 1994); and (b) K_γ computed for $N_{1,60cs} = 18.5$ blws/30 cm but varying CSR.

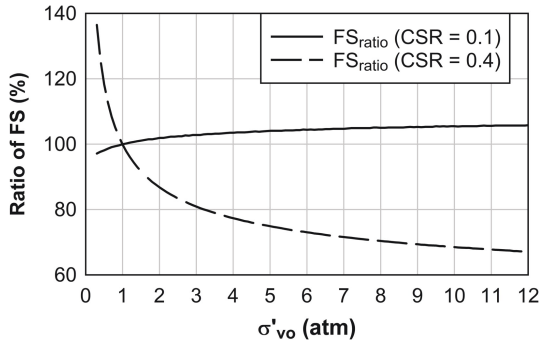

Fig. 14. Ratios of the computed FS for $CSR = 0.1$ and 0.4 using K_γ corresponding to $FS = 1$ to the FS for these $CSRs$ using K_γ corresponding to the "actual" FS for these $CSRs$.

(i.e., $FS_{K\sigma}/FS_{K\gamma}$ versus σ'_{vo}). As may be observed in this figure, the FS ratio for $CSR = 0.4$ ranges considerably more than when $CSR = 0.1$; this is because the CRR for the soil, 0.12, is closer to 0.1 than it is to 0.4. Accordingly, K_σ values computed per Eq. (1) using laboratory data may or may not be appropriate for the liquefaction triggering analyses for the project they were developed for, depending on the values of the CSR corresponding to the design earthquake ground motions for the project versus those corresponding to a $FS = 1$. This is particularly an issue when full probabilistic liquefaction hazard analyses are performed. In such cases a range of earthquake scenarios are considered (e.g., Green et al. 2020) and the range of seismic demand considered can differ considerably from the soil's resistance to liquefaction. In the case of Duncan Dam, if the design earthquake motions result in in-situ CSR values greater than 0.12, then the CSR/K_σ values used to analyze the dam were likely too high for conditions when $\sigma'_{vo} > 100$ kPa (~1 atm). For example, for $\sigma'_{vo} = 1{,}200$ kPa (~12 atm), the ratio of the FS computed using K_σ (i.e., the FS computed using K_γ corresponding to $FS = 1$) to the FS computed using K_γ (i.e., FS computed using K_γ corresponding to the "actual" FS) is only ~67% when $CSR = 0.4$. This could potentially lead to unnecessary and costly remediation of the foundation soils at large depths. In contrast, for denser soils (i.e., soils having a higher resistance to liquefaction triggering), the FS computed using K_σ may be overpredicted if the CSR for the design earthquake is considerably less than the CRR of the soil.

Comparison with Select K_σ Relationships

In an effort to explain the large scatter in K_σ data (e.g., Fig. 5), additional state variables such as D_r of the samples (e.g., Vaid and Sivathayalan 1996; Hynes and Olsen 1999), overconsolidation ratio (OCR) (e.g., Ishihara et al. 1978; Manmatharajan and Sivathayalan 2011; Montgomery et al. 2014), the State Parameter (ψ) (Jefferies and Been 2016), and the Relative State Parameter (ξ_R) (Boulanger 2003) have been considered. ξ_R is analogous to ψ (Been and Jefferies 1985) and is defined as the difference in D_r of the soil of interest and the corresponding D_r at critical state ($D_{r,cs}$) for the same σ'_{mo}, where $D_{r,cs}$ is estimated using the relationship proposed by Bolton (1986). However, both ψ and ξ_R are indices for the dilative/contractive tendencies of the soil at strains commensurate with critical state (i.e., large strains). In contrast, liquefaction triggering involves strains that are much smaller than those associated with critical state deformation (e.g., shear strains, γ, less than ~4% versus ~20% to reach critical state) and the contractive/dilative tendencies of soil varies significantly as a function of strain, up to critical state. This variation in the contractive/dilative tendencies as a function of strain is clearly illustrated in the curves shown in Figs. 7(b and c) (i.e., the vertical distance between the curves), where the curves shown in these figures are based on empirical regression of actual soil data (Ishibashi and Zhang 1993). Also, the difference in the strains relevant to liquefaction triggering versus critical state is essentially the issue identified by Seed and Lee (1966) when they found that the higher the σ'_o, the greater the number of stress cycles required to trigger liquefaction, all others factors being equal. They noted that this trend is opposite of what they expected based on critical state theory, not considering that the dilative/contractive tendencies of the soil varied as a function of strain. As a result, ξ_R does not adequately characterize the contractive/dilative tendencies of soil for the amplitude of the strains involved in liquefaction triggering, which will vary depending on the soil stiffness and the amplitude of the applied loading; the same holds for ψ. This is clearly illustrated in Fig. 1, in which all the liquefaction resistance curves shown are for samples that have the same ξ_R and ψ, but the cyclic resistance to liquefaction varies widely depending on sample preparation method (i.e., the stiffness of the samples is dependent on the preparation method, and thus different strains are induced in the differently prepared samples when the same CSR is applied). The proposed K_γ parameter inherently accounts for this variation in the contractive/dilative tendencies of soil via its dependency on soil stiffness (e.g., V_S) and the applied CSR, which in combination with the τ-γ response characteristics of the soil, results in an induced shear strain in the soil.

Many of the concepts underlying K_γ are similar to those used by Dobry and Abdoun (2015b) in developing their K_σ relationship. However, Dobry and Abdoun (2015b) developed their relationships for $FS = 1$, and also inherently assume that V_S is an accurate index for the cyclic resistance of soil to liquefaction (Dobry and Abdoun 2015a), independent of the soil's intrinsic properties (e.g., Fig. 3). In contrast, K_γ does not rely on any assumptions regarding the cyclic resistance to liquefaction, and the soil stiffness is used to relate the imposed τ (or CSR) to the induced γ. Because K_γ applies to the loading, it complements the use of penetration resistance as an index that accounts for the influence of intrinsic soil properties and soil state variables on the soil's cyclic resistance to liquefaction, CRR (e.g., Whitman 1971; Seed 1976, 1979).

Cetin and Bilge (2015) proposed an approach to account for simultaneous influence of initial effective confining stress, static stress bias, and shear stress reversal on the liquefaction resistance of soil that is also based on equating shear strains induced in a soil at a given stress state to the same soil at a reference stress state. Although the merit of accounting for the inter-relationship of the influence of these factors on liquefaction triggering is certainly intriguing, the focus herein is on their proposed relationship for accounting for the influence of initial effective confining stress on liquefaction triggering, absent of static stress bias and with full shear stress reversal. In the development of their procedure, Cetin and Bilge (2015) develop contours of constant induced shear strain in CSR-$n_{eq\tau}$ space for different initial effective confining stresses for a soil having a given D_r. These curves are analogous laboratory-based liquefaction curves where liquefaction triggering is defined using a γ criterion, as opposed to an r_u criterion (e.g., Ulmer et al. 2022). However, some of the curves developed by Cetin and Bilge are for γ that are considerably less than values commonly used to define liquefaction triggering in laboratory tests, and thus, are not "triggering" curves per se. From these contours, Cetin and Bilge develop K_σ curves corresponding to constant levels of γ per Eq. (1). Although the resulting K_σ curves proposed by Cetin and Bilge (2015) are based on equating shear strains induced in a soil at a given stress state to the same soil at a reference stress state, they are conceptually different from the K_γ-concept proposed herein.

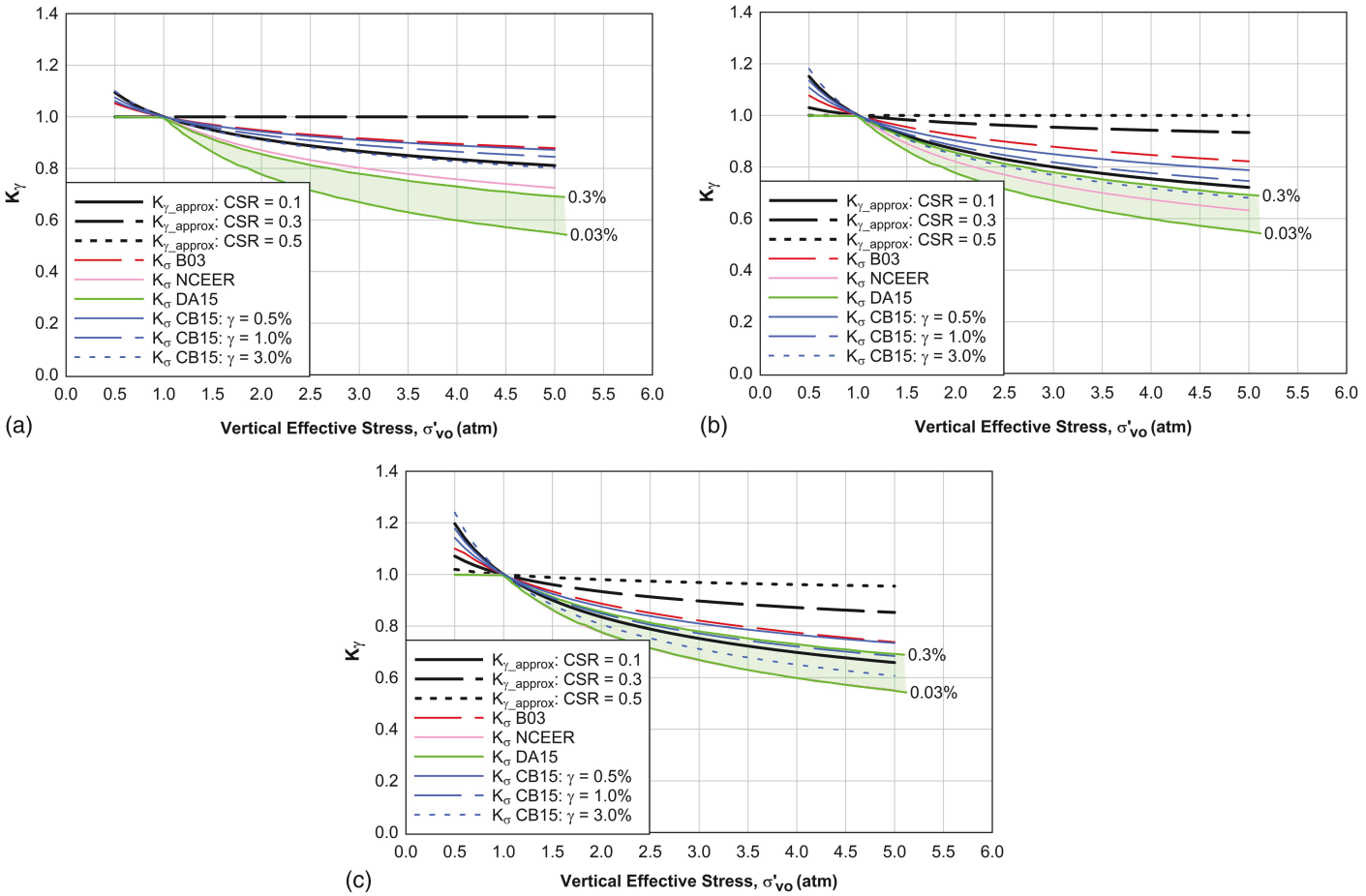

Fig. 15. Comparison of K_γ with the K_σ curves by NCEER 1997 [NCEER], Boulanger 2003 [B03], Dobry and Abdoun (2015b) [DA15], and Cetin and Bilge (2015) [CB15] for: (a) $q_{c1Ncs} = 57$ atm ($V_{S1} = 122$ m/s and $D_r = 33\%$); (b) $q_{c1Ncs} = 105$ atm ($V_{S1} = 164$ m/s and $D_r = 57\%$); and (c) $q_{c1Ncs} = 152$ atm ($V_{S1} = 197$ m/s and $D_r = 74\%$). The DA15 relationship is shown for $\gamma = 0.03\%$ to 0.3% and $K_o = 0.5$ to 1.0, although K_o has limited influence on the curves.

First, the underlying mechanics of their approach differs from that proposed herein (e.g., Cetin and Bilge inherently employs an effective stress framework, not a total stress framework in defining shear strain). Also, the laboratory test based contours of constant induced γ in CRR-$n_{eq\tau}$ space developed by Cetin and Bilge (2015) are inherently a function of the soil fabric and intrinsic soil properties, and it is uncertain whether this influence normalizes out in the computation of K_σ. Finally, it is uncertain what FS the Cetin and Bilge K_σ curves correspond to, where traditionally developed K_σ curves correspond to $FS = 1$ and the proposed K_γ relationship corresponds to the FS being evaluated in-situ.

A comparison of the proposed K_γ relationship (i.e., Fig. 8) and K_σ relationships proposed by NCEER (1997) [NCEER97], Boulanger (2003) [B03], Dobry and Abdoun (2015b) [DA15], and Cetin and Bilge (2015) [CB15] is presented in Fig. 15. Both the NCEER97 and B03 relationships are functions of the D_r (or penetration resistance of the soil), while the CB15 relationship is a function of both D_r and γ. Finally, the DA15 relationship is a function of γ and K_o, although Dobry and Abdoun (2015b) state that K_o has limited influence on their K_σ. Conceptually, the proposed K_γ relationship is most similar to the to DA15's K_σ relationship. However, unlike the DA15's K_σ relationship, a range for γ is not assumed a priori in the K_γ relationship but, rather, is determined from the V_S of the soil and the imposed CSR, with the IZ93 modulus reduction curves being used to represent the τ-γ response of the soil. Additionally, the K_γ considered in this paper is for normally consolidated soils, where K_o decreases with increasing density or penetration resistance [e.g., Eq. (6): Jaky 1944], not the opposite as assumed by Dobry and Abdoun (2015a). To allow a consistent comparison of the K_γ and K_σ relationships, consistent values of D_r, V_S, and q_{c1Ncs} were estimated using the relationship proposed by Idriss and Boulanger (2008) and Ulmer et al. (2020). As may be observed from Fig. 15, for a given penetration resistance the K_γ curves tend to be higher than the NCEER97, DA15, and CB15 K_σ relationships for $\sigma'_{vo} > \sim$100 kPa (1 atm), with this trend being more pronounced as CSR increases. In comparison with the B03 K_σ relationship, for a given penetration resistance K_γ tends to be lower for smaller values of CSR and higher for larger values of CSR for $\sigma'_{vo} > \sim$100 kPa (1 atm). This comparison highlights the significance of CSR on K_γ, which, as stated previously, is of particular relevance when full probabilistic liquefaction hazard analyses are performed in which a range of earthquake scenarios are considered (e.g., Green et al. 2020).

Final Miscellaneous Comments

Modulus Reduction Curves

As may be noted, the Ishibashi and Zhang (1993) modulus reduction curves are used in all the preceding analyses and discussions. The reason for this is that the functional form of the IZ93 equations

captures well the τ-γ response of the soil across all strains of interest. This is not the case for other commonly used modulus reduction curves that use a hyperbolic function as their base equation (e.g., Darendeli 2001; Menq 2003), where the application of large-strain strength correction factors commonly need to be applied (e.g., Yee et al. 2013). While the simple functional form of the modulus reduction curves used by Darendeli (2001) and Menq (2003), for example, may have advantages for use in site response analyses, which is their primary intended use, the authors found that the hyperbolic equation does not match well with laboratory liquefaction data. Alternative to empirical modulus reduction curves, advanced constitutive models could also be used to model the τ-γ response of the soil. However, as with the hyperbolic-based equations, constitutive models tend to work well over strain ranges specifically targeted in the calibration of the models based on their intended use and do not necessarily work well across the range of strains of interest to this study. As a result, the authors recommend the use of the IZ93 modulus reduction curves for computation of K_γ.

Overconsolidated Soils, Aged Soils, and Improved Sites

Other conditions where the K_γ-concept can resolve errors introduced by use of laboratory determined K_σ values is for over-consolidation sandy soils, aged sandy soils, and sandy soils remediated in a way that the in-situ lateral stresses are increased. However, these scenarios are not covered in this paper because of length restrictions and because overconsolidation sandy soils and improved sandy soil deposits require additional analysis to account for the influence of increased lateral stress on measured penetration resistance, in addition to how the increased lateral stress influences the K_γ factor used to normalize *CSR*. Full coverage of these topics will be presented in subsequent paper(s).

Use of K_γ with Current Triggering Models

As stated previously, K_γ should be used in place of K_σ in future-developed simplified stress-based triggering frameworks. However, K_γ should not be used in place of K_σ within existing simplified liquefaction evaluation procedures to assess liquefaction potential. This is because the *CRR* curves for existing triggering procedures are inherently based on K_σ relationships used in the development of those *CRR* curves. As a result, the K_γ relationships proposed herein can be used to analyze liquefaction case histories to develop new cyclic resistance ratio curves and/or to quantify the differences in K_σ versus K_γ to assess bias in K_σ relationships proposed by others, etc. Currently, a stress-based CPT simplified triggering model is being developed by the lead author and collaborators using the K_γ relationship proposed herein.

Conclusions

Intrinsic soil properties and soil state variables have long been known to influence liquefaction triggering. While variants of the stress-based procedure (i.e., penetration resistance and small-strain shear wave velocity, V_S, stress-based procedures) and the cyclic strain procedure have attractive attributes, each also has detractions. Proposed herein is an approach for incorporating the benefits of the V_S stress-based procedure and the cyclic strain procedure into the penetration test stress-based procedures, thus more properly and more mechanistically accounting for the influence of intrinsic soil properties and soil state variables on liquefaction triggering. This is achieved by normalizing cyclic stress ratio (*CSR*) by the K_γ factor. The proposed normalization factor, K_γ, should be used in place of K_σ. However, most previously proposed K_σ relationships were largely empirically-based K_σ, only accounted for the influence of the initial vertical effective stress (σ'_{vo}) on liquefaction triggering, and/or inherently assume that the *CSR* is equal to the cyclic resistance ratio (*CRR*) (i.e., the factor of safety, *FS*, against liquefaction triggering is equal to one). In contrast, K_γ is more mechanically based and accounts for the influence of σ'_{vo}, K_o, and soil fabric, and applies to all *FS*.

The underlying concept of the K_γ normalization factor is that when *CSR* is normalized by K_γ, the γ induced in a sample having the reference set of initial conditions [i.e., $\sigma'_{vo} \approx 100$ kPa (1 atm), lateral effective stress of a normally consolidated soil, and fabric consistent with a young soil deposit) should be the same as that, that would be induced in a similar sample having the actual initial conditions (i.e., σ'_{vo}, lateral effective stress, and soil fabric). The reason for this is that the relative movement of soil particles, which is requisite for breaking down the soil skeleton, generating excess pore water pressures, and triggering liquefaction, relates to the induced γ. However, the normalization of *CSR* by K_γ differs from the cyclic strain approach because it is couched in a total stress framework. The cyclic strain approach is inherently couched in an effective stress framework and, thus, carries with it the difficulties in relating the amplitude and duration of the shear strain loading parameters to earthquake ground motions.

The concept of equating the induced γ in a soil for a given set of initial reference conditions to that induced in the same soil for the actual set of initial conditions, inherently implies that K_γ is a function of the induced γ. This further distinguishes the K_γ normalization factor from the K_σ relationship proposed by Boulanger (2003) that correlates K_σ to the Relative State Parameter (ξ_R), where ξ_R is an index for the dilative/contractive tendencies of the soil at strains commensurate with critical state. Liquefaction triggering involves strains that are much smaller than those associated with critical state deformation, and the contractive/dilative tendencies of soil varies significantly as a function of strain, up to critical state. The proposed K_γ parameter inherently accounts for the variation of the contractive/dilative tendencies of soil by being a function of the applied *CSR*, which in combination with the τ-γ response characteristics of the soil, results in an induced γ in the soil. The τ-γ response characteristics of the soil is generically modeled herein, with good success, using the empirically based Ishibashi and Zhang (1993) [IZ93] modulus degradation curves.

The proposed K_γ factor should be used in place of K_σ in future-developed simplified triggering models. The K_γ relationship proposed herein are not intended to be used in conjunction with existing simplified liquefaction evaluation procedures to assess liquefaction potential. This is because the *CRR* curves for existing triggering procedures are inherently based on K_σ relationships used in the development of those *CRR* curves. As a result, the K_γ relationships proposed in this paper can be used to analyze liquefaction case histories to develop new cyclic resistance ratio curves and/or to quantify the differences in K_σ versus K_γ to assess bias in K_σ relationships proposed by others, etc.

Data Availability Statement

Some or all data, models, or code that support the findings of this paper are available from the corresponding author upon reasonable request.

Acknowledgments

This research was funded in part by the National Science Foundation (NSF) Grants CMMI-1825189 and CMMI-1937984.

This support is gratefully acknowledged. This study has also significantly benefited from enlightening discussions with Professor Misko Cubrinovski, University of Canterbury, Christchurch, New Zealand and review comments by Dr. Peter K. Robertson, Gregg Drilling & Testing Canada Ltd., and Dr. James K. Mitchell, Dr. Alba Yerro-Colom, Ms. Kaleigh Yost, Mr. Tyler Quick, and Mr. Tat Singh Thum from Virginia Tech. However, any opinions, findings, and conclusions or recommendations expressed in this paper are those of the authors and do not necessarily reflect the views of the NSF or others that are acknowledged.

Supplemental Materials

Eq. (S1) and Fig. S1 are available online in the ASCE Library (www.ascelibrary.org).

References

Alarcon-Guzman, A., J. L. Chameau, G. A. Leonards, and J. D. Frost. 1989. "Shear modulus and cyclic undrained behavior of sands." *Soils Found.* 29 (4): 105–119. https://doi.org/10.3208/sandf1972.29.4_105.

Andrus, R. D., K. H. Stokoe II, and H. Juang. 2004. "Guide for shear-wave-based liquefaction potential evaluation." *Earthquake Spectra* 20 (2): 285–308. https://doi.org/10.1193/1.1715106.

Baxter, C. P. D., A. S. Bradshaw, R. A. Green, and J.-H. Wang. 2008. "Correlation between cyclic resistance and shear-wave velocity for providence silts." *J. Geotech. Geoenviron. Eng.* 134 (1): 37–46. https://doi.org/10.1061/(ASCE)1090-0241(2008)134:1(37).

Been, K., and M. G. Jefferies. 1985. "A state parameter for sands." *Géotechnique* 35 (2): 99–112. https://doi.org/10.1680/geot.1985.35.2.99.

Bolton, M. D. 1986. "The strength and dilatancy of sands." *Géotechnique* 36 (1): 65–78. https://doi.org/10.1680/geot.1986.36.1.65.

Boulanger, R. W. 2003. "High overburden stress effects in liquefaction analyses." *J. Geotech. Geoenviron. Eng.* 129 (12): 1071–1082. https://doi.org/10.1061/(ASCE)1090-0241(2003)129:12(1071).

Boulanger, R. W., and I. M. Idriss. 2014. *CPT and SPT based liquefaction triggering procedures*. Rep. No. UCD/CGM-14/01. Davis, CA: Center for Geotechnical Modelling, Dept. of Civil and Environmental Engineering, Univ. of California, Davis.

Bradshaw, A. S., and C. D. P. Baxter. 2007. "Sample preparation of silts for liquefaction testing." *Geotech. Test. J.* 30 (4): 324–332.

Byrne, P. M. 1991. "A cyclic shear-volume coupling and pore pressure model for sand." In *Proc., 2nd Int. Conf. on Recent Advances in Geotechnical Earthquake Engineering and Soil Dynamics*, edited by S. Prakash, 47–55. St. Louis, MO: University of Missouri Rolla Press.

Castro, G. 1975. "Liquefaction and cyclic mobility of sands." *J. Geotech. Eng. Div.* 101 (6): 551–569. https://doi.org/10.1061/AJGEB6.0000173.

Cetin, K. O., and H. T. Bilge. 2015. "Stress scaling factors for seismic soil liquefaction problems." In *Perspectives on earthquake geotechnical engineering in Honor of Prof. Kenji Ishihara*, edited by A. Ansal and M. Sakr, 113–139. Cham, Switzerland: Springer International Publishing.

Cetin, K. O., R. B. Seed, A. Der Kiureghian, K. Tokimatsu, L. F. Harder Jr., R. E. Kayen, and R. E. S. Moss. 2004. "SPT-based probabilistic and deterministic assessment of seismic soil liquefaction potential." *J. Geotech. Geoenviron. Eng.* 130 (12): 1314–1340. https://doi.org/10.1061/(ASCE)1090-0241(2004)130:12(1314).

Cetin, K. O., R. B. Seed, R. E. S. Moss, A. Der Kiureghian, K. Tokimatsu, L. F. Harder Jr., and R. E. Kayen. 2000. *Field case histories for SPT-based in situ liquefaction potential evaluation*. PEER Rep. No. UCB/GT-2000/09. Berkeley, CA: Pacific Earthquake Engineering Research, Univ. of California at Berkeley.

Darendeli, M. 2001. "Development of a new family of normalized modulus reduction and material damping curves." Ph.D. dissertation, Dept. of Civil, Architectural, and Environmental Engineering, Univ. of Texas at Austin.

Dobry, R., and T. H. Abdoun. 2015a. "3rd Ishihara lecture: An investigation into why liquefaction charts work: A necessary step toward integrating the states of art of practice." *Soil Dyn. Earthquake Eng.* 68 (Jan): 40–56. https://doi.org/10.1016/j.soildyn.2014.09.011.

Dobry, R., and T. H. Abdoun. 2015b. "Cyclic shear strain needed for liquefaction triggering and assessment of overburden pressure factor $K\sigma$." *J. Geotech. Geoenviron. Eng.* 141 (11): 04015047. https://doi.org/10.1061/(ASCE)GT.1943-5606.0001342.

Dobry, R., R. Ladd, F. Yokel, R. Chung, and D. Powell. 1982. *Prediction of pore water pressure buildup and liquefaction of sands during earthquakes by the cyclic strain method. NBS Building Science Series 138*. Washington, DC: National Bureau of Standards.

Dobry, R., K. H. Stokoe II, R. S. Ladd, and T. L. Youd. 1981. "Liquefaction susceptibility from S-Wave velocity." In *Proc., ASCE National Convention: Situ Tests to Evaluate Liquefaction Susceptibility.* Reston, VA: ASCE.

Finn, W. D. L., D. J. Pickering, and P. L. Bransby. 1971. "Sand liquefaction in triaxial and simple shear tests." *J. Soil Mech. Found. Div.* 97 (4): 639–659. https://doi.org/10.1061/JSFEAQ.0001579.

Green, R. A., et al. 2020. "Liquefaction hazard in the groningen region of the netherlands due to induced seismicity." *J. Geotech. Geoenviron. Eng.* 146 (8): 04020068. https://doi.org/10.1061/(ASCE)GT.1943-5606.0002286.

Green, R. A., J. J. Bommer, A. Rodriguez-Marek, B. Maurer, P. Stafford, B. Edwards, P. P. Kruiver, G. de Lange, and J. van Elk. 2019. "Addressing limitations in existing 'simplified' liquefaction triggering evaluation procedures: Application to induced seismicity in the groningen gas field." *Bull. Earthquake Eng.* 17 (8): 4539–4557. https://doi.org/10.1007/s10518-018-0489-3.

Green, R. A., M. Cubrinovski, B. Cox, C. Wood, L. Wotherspoon, B. Bradley, and B. Maurer. 2014. "Select liquefaction case histories from the 2010–2011 Canterbury earthquake sequence." *Earthquake Spectra* 30 (1): 131–153. https://doi.org/10.1193/030713EQS066M.

Green, R. A., and W. F. Marcuson III. 2014. "The $\varphi = 0$ concept: Review of its theoretical basis and pragmatic issues with its implementation." In *Geo-Congress 2014: From soil behavior fundamentals to innovations in geotechnical engineering, Honoring Roy E. Olson*, Geotechnical Special Publication 233, edited by M. Iskander, J. E. Garlanger, and M. H. Hussein, 308–321. Reston, VA: ASCE.

Green, R. A., and E. Rodriguez-Arriaga. 2019. "Assessment of an alternative implementation of the Dobry et al. cyclic strain procedure for evaluating liquefaction triggering." In *Proc., Earthquake Geotechnical Engineering for Protection and Development of Environment and Constructions*, edited by Silvestri and Moraci. Rome: Associazione Geotecnica Italiana.

Hardin, B. O., and F. E. Richart Jr. 1963. "Elastic wave velocities in granular soils." *J. Soil Mech. Found. Div.* 89 (1): 33–65. https://doi.org/10.1061/JSFEAQ.0000493.

Hayati, H., and R. D. Andrus. 2009. "Updated liquefaction resistance correlation factors for aged sands." *J. Geotech. Geoenviron. Eng.* 135 (11): 1683–1692. https://doi.org/10.1061/(ASCE)GT.1943-5606.0000118.

Hynes, M. E., and R. Olsen. 1999. "Influence of confining stress on liquefaction resistance." *Proc., Int. Symp. on the Physics and Mechanics of Liquefaction*, 145–152. Rotterdam, Netherlands: A.A. Balkema.

Idriss, I. M., and R. W. Boulanger. 2008. *Soil liquefaction during earthquakes*. EERI Publication, Monograph MNO-12. Oakland, CA: Earthquake Engineering Research Institute.

Ishibashi, I., and X. Zhang. 1993. "Unified dynamic shear moduli and damping ratios of sand and clay." *Soils Found.* 33 (1): 182–191. https://doi.org/10.3208/sandf1972.33.182.

Ishihara, K., S. Iwamoto, S. Yasuda, and H. Takatsu. 1977. "Liquefaction of anisotropically consolidated sand." In Vol. 2 of *Proc., 9th Int. Conf. on Soil Mechanics and Foundation Engineering*, 261–264. London: International Society for Soil Mechanics and Geotechnical Engineering.

Ishihara, K., M. Sodekawa, and Y. Tanaka. 1978. "Effects of overconsolidation on." In *Liquefaction characteristics of sands containing fines, STP 654*, 246–264. West Conshohocken, PA: ASTM.

Jaky, J. 1944. "The coefficient of earth pressure at rest (in Hungarian: A Nyugalmi Nyomas Tenyezoje)." *J. Soc. Hungarian Eng. Archit. (Magyar Mernok es Epitesz-Egylet Kozlonye)* 355–358.

Jefferies, M., and K. Been. 2016. *Soil liquefaction: A critical state approach*. 2nd ed. Boca Raton, FL: CRC Press.

Kayen, R., R. E. S. Moss, E. M. Thompson, R. B. Seed, K. O. Cetin, A. Der Kiureghian, Y. Tanaka, and K. Tokimatsu. 2013. "Shear-wave velocity–based probabilistic and deterministic assessment of seismic soil liquefaction potential." *J. Geotech. Geoenviron. Eng.* 139 (3): 407–419. https://doi.org/10.1061/(ASCE)GT.1943-5606.0000743.

Lasley, S. J., R. A. Green, and A. Rodriguez-Marek. 2016. "New stress reduction coefficient relationship for liquefaction triggering analyses." *J. Geotech. Geoenviron. Eng.* 142 (11): 06016013. https://doi.org/10.1061/(ASCE)GT.1943-5606.0001530.

Lasley, S. J., R. A. Green, and A. Rodriguez-Marek. 2017. "Number of equivalent stress cycles for liquefaction evaluations in active tectonic and stable continental regions." *J. Geotech. Geoenviron. Eng.* 143 (4): 04016116. https://doi.org/10.1061/(ASCE)GT.1943-5606.0001629.

Lee, K. L., and H. B. Seed. 1967. "Cyclic stress conditions causing liquefaction of sands." *J. Soil Mech. Found. Div.* 93 (1): 47–70. https://doi.org/10.1061/JSFEAQ.0000945.

Manmatharajan, V., and S. Sivathayalan. 2011. "Effect of overconsolidation on cyclic resistance correction factors Ks and Ka." In *Proc., 14th Pan-American Conf. on Soil Mechanics and Geotechnical Engineering, and the 64th Canadian Geotechnical Conf.* Richmond, BC, Canada: Canadian Geotechnical Society.

Martin, G. R., W. D. L. Finn, and H. B. Seed. 1975. "Fundamentals of liquefaction under cyclic loading." *J. Geotech. Eng. Div.* 101 (5): 423–438. https://doi.org/10.1061/AJGEB6.0000164.

Menq, F.-Y. 2003. "Dynamic properties of sandy and gravelly soils." Ph.D. dissertation, Dept. of Civil, Architectural, and Environmental Engineering, Univ. of Texas at Austin.

Mitchell, J. K., and K. Soga. 2005. *Fundamentals of soil behavior*. 3rd ed. Hoboken, NJ: Wiley.

Montgomery, J., R. W. Boulanger, and L. F. Harder Jr. 2014. "Examination of the Ks overburden correction factor on liquefaction resistance." *J. Geotech. Geoenviron. Eng.* 140 (12): 04014066. https://doi.org/10.1061/(ASCE)GT.1943-5606.0001172.

Moss, R. E. S., R. B. Seed, R. E. Kayen, J. P. Stewart, T. L. Youd, and K. Tokimatsu. 2003. *Field case histories for CPT-based in situ liquefaction potential evaluation*. Geoengineering Research Rep. No. UCB/GE-2003/04. Berkeley, CA: Univ. of California at Berkeley.

Mulilis, J. P., C. K. Chan, and H. B. Seed. 1975. *The effects of method sample preparation on the cyclic stress-strain behavior of sands*. Rep. No. EERC 75-18. Berkeley, CA: Earthquake Engineering Research Center, Univ. of California at Berkeley.

Mulilis, J. P., H. B. Seed, C. K. Chan, J. K. Mitchell, and K. Arulanandan. 1977. "Effects of sample preparation on sand liquefaction." *J. Geotech. Eng. Div.* 103 (GT2): 91–108.

NCEER (National Center for Earthquake Engineering Research). 1997. *Proceedings of the NCEER workshop on evaluation of liquefaction resistance of soils*. Technical Report NCEEE-97-0022. Buffalo, NY: National Center for Earthquake Engineering Research, State University of New York at Buffalo.

Pillai, V. S., and P. M. Byrne. 1994. "Effect of overburden pressure on liquefaction resistance of sand." *Can. Geotech. J.* 31 (1): 53–60. https://doi.org/10.1139/t94-006.

Polito, C. P., and J. R. Martin II. 2003. "A reconciliation of the effects of non-plastic fines on the liquefaction resistance of sands reported in the literature." *Earthquake Spectra* 19 (3): 635–651. https://doi.org/10.1193/1.1597878.

Richart, F. E., Jr., J. R. Hall, and R. D. Woods. 1970. *Vibrations of soils and foundations*. Englewood Cliffs, NJ: Prentice Hall.

Robertson, P. K. 2015. "Comparing CPT and *Vs* liquefaction triggering methods." *J. Geotech. Geoenviron. Eng.* 141 (9): 04015037. https://doi.org/10.1061/(ASCE)GT.1943-5606.0001338.

Rodriguez-Arriaga, E., and R. A. Green. 2018. "Assessment of the cyclic strain approach for evaluating liquefaction triggering." *Soil Dyn. Earthquake Eng.* 113 (Oct): 202–214. https://doi.org/10.1016/j.soildyn.2018.05.033.

Salgado, R., R. W. Boulanger, and J. K. Mitchell. 1997. "Lateral stress effects on CPT liquefaction resistance correlations." *J. Geotech. Geoenviron. Eng.* 123 (8): 726–735. https://doi.org/10.1061/(ASCE)1090-0241(1997)123:8(726).

Seed, H. B. 1976. "Evaluation of soil liquefaction effects on level ground during earthquakes." In *Liquefaction problems in geotechnical engineering, ASCE annual convention and exposition*, 1–104. Reston, VA: ASCE.

Seed, H. B. 1979. "Soil liquefaction and cyclic mobility evaluation for level ground during earthquakes." *J. Geotech. Eng. Div.* 105 (2): 201–255. https://doi.org/10.1061/AJGEB6.0000768.

Seed, H. B. 1983. "Earthquake resistant design of earth dams." In *Proc., Symp. on Seismic Design of Embankments and Caverns*, 41–64. Reston, VA: ASCE.

Seed, H. B., and I. M. Idriss. 1970. *Soil moduli and damping factors for dynamic response analyses*. Rep. No. EERC 70-10. Berkeley, CA: Earthquake Engineering Research Center, Univ. of California at Berkeley.

Seed, H. B., and I. M. Idriss. 1971. "Simplified procedure for evaluating soil liquefaction potential." *J. Soil Mech. Found. Div.* 97 (9): 1249–1273. https://doi.org/10.1061/JSFEAQ.0001662.

Seed, H. B., and K. L. Lee. 1966. "Liquefaction of saturated sands during cyclic loading." *J. Soil Mech. Found. Div.* 92 (6): 105–134. https://doi.org/10.1061/JSFEAQ.0000913.

Seed, H. B., K. L. Lee, I. M. Idriss, and F. Makdisi. 1973. *Analysis of the slides in the San Fernando Dams during the Earthquake of Feb. 9, 1971*. Report No. EERC 73-2. Berkeley, CA: Earthquake Engineering Research Center, Univ. of California at Berkeley.

Seed, H. B., and W. H. Peacock. 1971. "Test procedures for measuring soil liquefaction characteristics." *J. Soil Mech. Found. Div.* 97 (8): 1099–1119. https://doi.org/10.1061/JSFEAQ.0001649.

Seed, R. B., and L. F. Harder Jr. 1989. "SPT-based analysis of cyclic pore pressure generation and undrained residual strength." In *Proc., Seed Memorial Symp.*, edited by J. M. Duncan, 351–376. Vancouver, BC, Canada: BiTech.

Silver, M. L., and H. B. Seed. 1971. "Volume changes in sand during cyclic loading." *J. Soil Mech. Found. Div.* 97 (SM9): 1171–1180.

Stokoe, K. H., II, J. M. Roesset, J. G. Bierschwale, and M. Aouad. 1988. "Liquefaction potential of sands from shear wave velocity." In *Proc., 9th World Conf. on Earthquake Engineering*, 213–218. Tokyo: International Association for Earthquake Engineering.

Tokimatsu, K., and A. Uchida. 1990. "Correlation between liquefaction resistance and shear wave velocity." *Soils Found.* 30 (2): 33–42. https://doi.org/10.3208/sandf1972.30.2_33.

Tokimatsu, K., T. Yamazaki, and Y. Yoshimi. 1986. "Soil liquefaction evaluations by elastic shear moduli." *Soils Found.* 26 (1): 25–35. https://doi.org/10.3208/sandf1972.26.25.

Tokimatsu, K., and Y. Yoshimi. 1983. "Empirical correlation of soil liquefaction based on SPT N-values and fines content." *Soils Found.* 23 (4): 56–74. https://doi.org/10.3208/sandf1972.23.4_56.

Ulmer, K. J., R. A. Green, and A. Rodriguez-Marek. 2020. "A consistent correlation between vs, spt, and cpt metrics for use in liquefaction evaluation procedures." In *Geo-Congress 2020: Geotechnical Earthquake Engineering and Special Topics*, Geotechnical Special Publication 318, edited by J. P. Hambleton, R. Makhnenko, and A. S. Budge, 132–140. Reston, VA: ASCE.

Ulmer, K. J., R. A. Green, and A. Rodriguez-Marek. 2022. "Recommended b-value for computing number of equivalent cycles and magnitude scaling factors for simplified liquefaction triggering evaluation procedures." *J. Geotech. Geoenviron. Eng.*

Vaid, Y. P., and S. Sivathayalan. 1996. "Static and cyclic liquefaction potential of Fraser Delta sand in simple shear and triaxial tests." *Can. Geotech. J.* 33 (2): 281–289. https://doi.org/10.1139/t96-007.

Verdugo, R. 2016. "Experimental and conceptual evidence about the limitations of shear wave velocity to predict liquefaction." *Soil Dyn. Earthquake Eng.* 91 (Dec): 160–174. https://doi.org/10.1016/j.soildyn.2016.09.046.

Wair, B. R., J. T. DeJong, and T. Shantz. 2012. *Guidelines for estimation of shear wave velocity profiles*. PEER Rep. 2012/08. Berkeley, CA: Pacific Earthquake Engineering Research Center.

Wang, J.-H., K. Moran, and C. D. P. Baxter. 2006. "Correlation between cyclic resistance ratios of intact and reconstituted offshore saturated sands and silts with the same shear wave velocity." *J. Geotech. Geoenviron. Eng.* 132 (12): 1574–1580.

Whitman, R. V. 1971. "Resistance of soil to liquefaction and settlement." *Soils Found.* 11 (4): 59–68. https://doi.org/10.3208/sandf1960.11.4_59.

Wood, C. M., B. R. Cox, R. A. Green, L. Wotherspoon, B. A. Bradley, and M. Cubrinovski. 2017. "Vs-based evaluation of select liquefaction case histories from the 2010-2011 Canterbury earthquake sequence." *J. Geotech. Geoenviron. Eng.* 143 (9): 04017066. https://doi.org/10.1061/(ASCE)GT.1943-5606.0001754.

Yee, E., J. P. Stewart, and K. Tokimatsu. 2013. "Elastic and large-strain nonlinear seismic site response from analysis of vertical array recordings." *J. Geotech. Geoenviron. Eng.* 139 (10): 1789–1801. https://doi.org/10.1061/(ASCE)GT.1943-5606.0000900.

Yi, F. 2010. "Procedure to evaluate liquefaction-induced lateral spreading based on shear wave velocity." In *Proc., 5th Int. Conf. on Recent Advances in Geotechnical Earthquake Engineering and Soil Dynamics*, edited by S. Prakash. Rolla, MO: University of Missouri Rolla Press.

Youd, T. L., et al. 2001. Liquefaction resistance of soils: Summary report from the 1996 NCEER and 1998 NCEER/NSF workshops on evaluation of liquefaction resistance of soils." *J. Geotech. Geoenviron. Eng.* 127 (10): 817–833. https://doi.org/10.1061/(ASCE)1090-0241(2001)127:10(817).